Edge analysis of seasonal variability in chlorophyll maps of the Black Sea

by

Ashwini G. Deshpande

Submitted to the Department of Earth, Atmospheric, and Planetary
Science
in partial fulfillment of the requirements for the degree of

Master of Science

at the

MASSACHUSETTS INSTITUTE OF TECHNOLOGY

June 2000

© Ashwini G. Deshpande, MM. All rights reserved.

The author hereby grants to MIT permission to reproduce and
distribute publicly paper and electronic copies of this thesis document
in whole or in part.

Author ....
Department of Earth, Atmospheric, and Planetary Science
May 5, 2000

Certified by...
Paola Malanotte-Rizzoli
Professor
Thesis Supervisor

Accepted by ....
Ronald Prinn
Chairman, Department of Earth, Atmospheric, and Planetary Science

Edge analysis of seasonal variability in chlorophyll maps of the Black Sea

by

Ashwini G. Deshpande

Abstract

The use of remotely sensed oceanographic data would be greatly benefitted by being able to detect circulation features automatically through edge detection. In the Black Sea, the use of edge detection to identify fronts can be used to study the effects of river input on circulation patterns and biological and physical interactions. The use of edge detection on remotely sensed chlorophyll data is limited by noisy data, inaccurate measurements, temporal and spatial gaps in data, and limitations on computational power. The algorithm described in this thesis utiliizes image processing techniques to create an edge detection process that shows the effects of the Danube river input on Black Sea circulation patterns with little computational complexity.

Thesis Supervisor: Paola Malanotte-Rizzoli
Title: Professor

Acknowledgments

I would like to acknowledge my advisor, Paola Malanotte-Rizzoli and Temel Oguz for all their support, technical advice and guidance throughout this project. I would also like to thank the Distributed Active Archive Center (Code 902) at the Goddard Space Flight Center for the distribution of these data. The SeaWiFS project (Code 970.2) at NASA Goddard also deserves thanks, both for the production of the data used for this thesis and for encouraging my interest in oceanography. These activities are sponsored by NASA's Mission to Planet Earth Program.

My sincerest gratitude also goes out to the AAAS ACCESS program and Laureen Summers, Mike Hartman, and Dan Krieger. Also, I would like to thank Bob Caffrey of NASA Goddard for never making (or letting) me decide what I wanted to do and for his valuable advice.

My family deserves appreciation for their patience and support. My brother, Akshay Deshpande, who has always set a good example and has been the staunchest competition. I would also like to thank my sister, Chinmayee Kale, for her unwaivering love. My parents, of course, deserve my strongest recognition for their sacrifices and unconditional love.

Finally, I would like to recognize the good friends I've made at MIT for constantly harrassing, goading, teasing, and provoking me . . . and making me happy that I came.

Contents

List of Figures

List of Tables

Chapter 1

Introduction

The Black Sea is a unique environment that has historically hosted a wide diversity of creatures. In the second half of this century, its ecosystem has decayed as a result of anthropogenic influence. Since the magnitude of problem and its effects on the community surrounding the sea are profound, there is considerable research effort to understand the dynamics of changes that the Black Sea is undergoing.

One of the factors that is causing the decline of the sea is pollution from rivers entering the Black Sea. These rivers often carry high nutrient loads that cause large algae blooms in the sea. The decay of these blooms causes eutrophication. Being able to understand and observe the effects of river pollution on the biological and physical interactions of the Black Sea can offer insight into its changing ecology.

Remote sensing of ocean color allows a unique opportunity to do this. Ocean color data estimate primary productivity and chlorophyll by comparing the amount of light reflected at several wavelengths that correspond to color. This color is given to water by sediments and biological productivity in water. Obtaining such measurements from space creates data sets with high temporal and spatial resolution which is critical when studying small time frame changes.

Despite its clear benefits, remote sensing data also has problems that must be addressed in order to use the data. One is the sheer volume of data that must be analyzed. In order to do a two summer study, nearly 300 data files must be examined. Detecting features of interest by hand can be a long, laborious, and inaccurate process.

Developing means to automatically detect these features will make the use of remote sensing data more feasible.

Edge detection is one possibility for automatic feature detection. Algorithms search images to find areas of change. In chlorophyll maps, these areas correspond to fronts and circulation features. The edge detection algorithm developed for this thesis is one that requires little computational power and has reasonable accuracy. The further development of this algorithm and improvements to it could make it an efficient means of automatic feature detection.

Chapter 2

The Black Sea

2.1 Geography

The Black Sea is located between Europe and Asia Minor. It is an inland sea that is connected to the ocean only through the Mediterranean. More than sixteen million people live in the coastal areas of the six countries that border the sea — Bulgaria, Georgia, Romania, the Russian Federation, Turkey, and the Ukraine. A map of the region can be seen in Figure 2-1. However, with a catchment area of more than 2 million square kilometers, the health of the Black Sea affects more than 22 countries. [17]

The recent decline of the sea due to pollution has been attributed to many sources. Both international rivers and coastal pollution are to blame. This leaves a large number of countries – many of which are still developing during the post-cold war era – responsible for controlling the factors that cause the decay of the Black Sea. [17]

2.2 Water Balance

The black sea has a surface area of 423,000 km^2 and contains 547,000 km^3 of water. It has regions of brackish, marine, and fresh water. The major components in the water balance are river discharge, precipitation, evaporation, marine exchange via the Bosphorus and Kerch straits. Changes in any of these sources strongly affect the
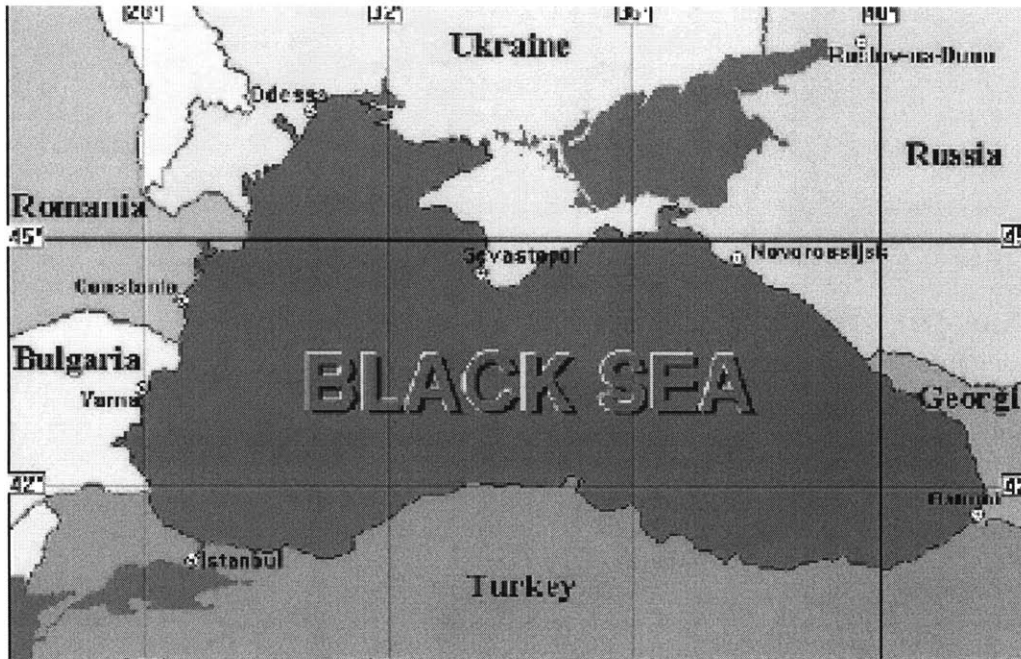
Figure 2-1: This is a map of the Black Sea region. Several countries border the Black Sea. However, the health of the Sea effects many more nations. [14]

unique Black Sea water balance.

2.2.1 Rivers

The largest volume of river flow into Black Sea comes from the North-western coast. The primary rivers contributing to this flow are the Danube, the Dniester, the Dnieper, and the Southern Bug. Rivers in the Northwest region contribute an average 389 km^3 of water into the sea in 1970. With an average flux of 208 km^3 of water per year, the Danube river is the strongest source of river water in the Northwestern region of the Black Sea.

The northwest region is also very shallow. It is particularly sensitive to changes in water balance. Flow changes in the rivers of that region affect the salt/freshwater balance. The nutrient flux of these rivers also drive changes in the biological activity of this region. The premise behind this project is that changes in circulation patterns driven by changes in river runoff can be observed through biological changes.

2.2.2 Precipitation

Another freshwater source is precipitation. An average of 225 km^3 of precipitation falls over the Black Sea each year. The primary source of this rainfall is atmospheric cyclonic activity that moves from west to east in the southern Black Sea. In the northwestern section of the sea, summer precipitation is also a considerable source. While the total precipitation over the Black Sea is much smaller than the river input, the precipitation varies considerably and causes seasonal and yearly changes in the water balance.

2.2.3 Evaporation

Over the past fifty years, the amount of water being evaporated from the sea is decreasing. In 1951, 484 km^3 of water were evaporated from the sea. In 1985, only 289 km^3 were evaporated from the sea. This phenomenon is attributed to changes in wind properties.

2.2.4 Marine Exchange

Marine water is exchanged through the Bosphorus and the Kerch Straits. Between 123 km^3 per year and 312 km^3 per year of water flow into the Black Sea through the Bosphorus. While the amount is varying, most scientists agree that there is twice as much outflow through the Bosphorus. The Kerch strait has an inflow of between 22 km^3 per year and 95 km^3 per year. The outflow through this straight is between 29 km^3 per year and 70 km^3 per year

The average fresh water balance in the Black Sea is positive. It varies seasonally being negative in the winter months. The driving force in these changes is fluctuations in river discharge.

2.3 Ecological Concerns

There is a considerable amount of interest in the Black Sea's ecological deterioration. During the second half of this century the condition of the Sea has deteriorated considerably. This is driven by many factors such as an increased presence of phytoplanktonic blooms, the introduction of exotic species into the ecosystem, and changes in the chemical structure of the sea.

2.3.1 Eutrophication

Anthropogenic eutrophication has caused phenomena such as decreases in biological diversity, population bursts of select species, declining water transparency, hypoxia in bottom waters, and mass mortalities of zoobenthos and nektobenthos fish. These problems are all caused by a sharp increase in the mineral content of run off into the Black Sea. The Black Sea is one of the worst examples of the effects of excessive water fertilization.

The major sources of nutrient flux into the sea are agricultural fertilizers, sewage, discharges from animal husbandry, and atmospheric fallout. The domination of these sources varies by location. In the Northwestern Black Sea, this processes can be strongly linked to the increases in nutrients in river discharge. The Danube, Dniester, and Dnieper rivers carried 14,000 tons of phosphates and 155,000 tons of nitrates in the 1950's. In the 1980's, these quantities increased to 55,000 tons of phosphates and 340,000 tons of nitrates.

Eutrophication affects the diversity of phytoplankton. The process stimulates the growth of dinoflagellates and inhibits the growth of diatoms. This process then indirectly affects zooplankton by increasing its volume if the zooplankton feasts on species that are stimulated by eutrophication.

The problem of hypoxia is also indirectly affected by eutrophication. The death of the massive blooms caused by eutrophication uses oxygen resources to oxidize organic matter. This process has also reduces the biological diversity of the Black Sea by decreasing the amount of available oxygen in shallow shelf waters.

2.3.2 Hypoxic Water

The morphometry and water balance of the sea has created a a water volume that is nearly 87 percent anoxic. Of the oxygenated water, only 13 percent is shallow surface and shelf water. Figure 2-2 shows the distribution of anoxic water in the Black Sea. The eutrophication problem puts the small amount of oxygenated water in the shelves and coastal areas under severe stress.

The zones of hypoxia in the sea have grown throughout the past several decades. Between 1973 and 1990 the affected bottom area increased from 3500 km^2 to 40,000 km^2. In the north-western shelf, which is 64,000 km^2, the area of hypoxia has extended over a significant portion of the shelf area. This lack of oxygen has led to the death of 5 million tons of fish between 1972 and 1990. [17]

2.3.3 Exotic species

Another strong anthropogenic influence in the Black Sea is the introduction of non-native species. Since the Black Sea hosts a diverse variety of habitats, it is particularly susceptible to this problem. One of the most common ways that invader species enter the sea is on ocean-going ships.

Some species attach themselves to the hulls of ships. These organisms vary in size and include everything from fish to shrimp to algae. Some of these organisms attach themselves to the living matter on the hull. More mobile organisms hide between the barnacles when the ship is in motion to avoid being swept away by the current.

Ballast tanks are also a large cause of this problem. Water is pumped into these tanks to stabilize it when there is no cargo. When ships fill these tanks, suspended matter and planktonic organisms are also pumped into the tanks. Without inspections, this water is dumped into the sea upon arrival. Organisms which survive the journey can become naturalized to the new system.

While the Black Sea has a long history of exotic species invading its water, recently much of the focus has been on *Mnemiopsis Leidyi*, shown in Figure 2-3. In the early 1980's this jelly fish was introduced to the Black Sea by ships from the atlantic coast of
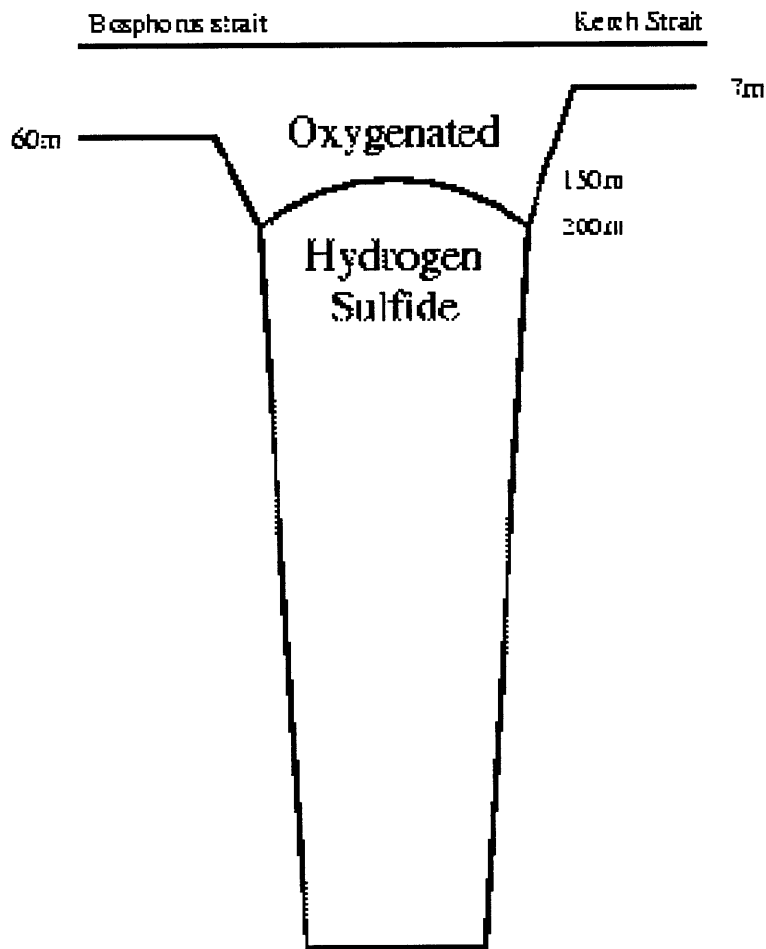
Figure 2-2: This figure shows the wide spread presence of anoxic water in the Black Sea. The increasing size of this area is of considerable ecological concern. [17]
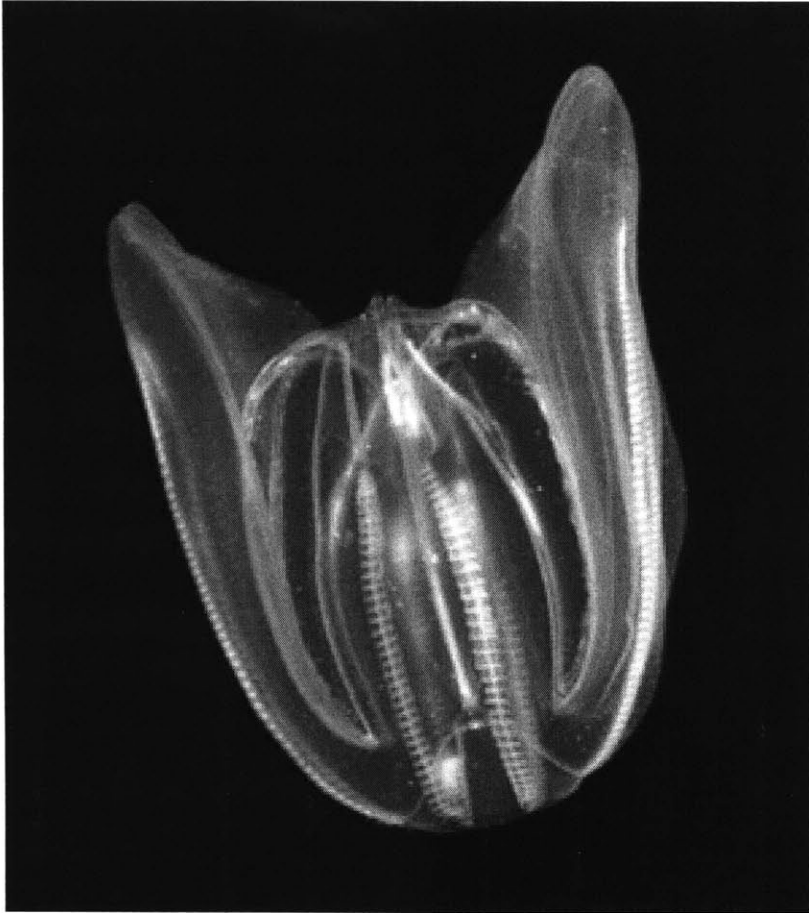
Figure 2-3: A single adult *Mnemiopsis Leidyi* [9].

North America. By the late 1980's, it's total biomass was estimated at 1,000,000,000 tons. It feeds on zooplankton, fish larvae, and pelagic eggs. The *Mnemiopsis Leidyi* has depleted commercial fish stocks by depriving the fish of zooplankton and by eating their eggs and larvae. Its effects of zooplankton population can be seen in Figure 2-4. This has given a profound economic blow to the Black Sea region. [17]
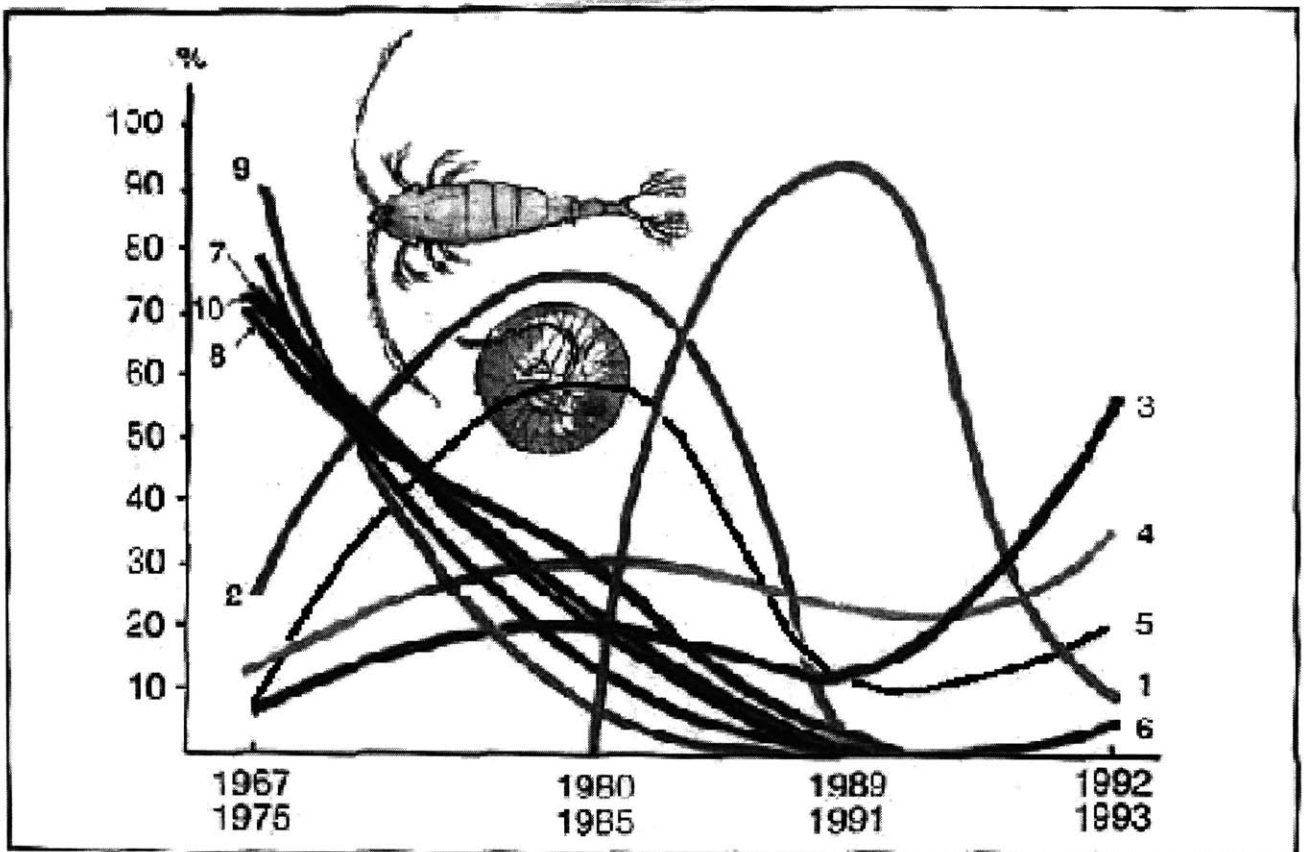
Figure 2-4: This figure shows the decline of several zooplankton species follow-inf the rise of the *Mnemiopsis Leidyi*(1) in the Black Sea. 1.*Mnemiopsis Leidyi* 2.*Oithona minuta* 3.*Pleopis polyphemoides* 4.*Acartia clausia* 5.*Noctiluca scintillans* 6.*Pontella mediterranea* 7.*Penilia avirostris* 8.*Paracalanus parvus* 9.*Labidocera brunescens* 10.*Centropages kroyeri pontica* [17]

Chapter 3

Circulation Features

The oceanographic characteristics of the Black Sea have become rather well known in recent years. Since the 1980's, in fact, intense field work has been underway to characterize it. The increasing number of observatories, modeling studies and the analysis of satellite imagery have rapidly contributed to this new knowledge. [12]

The Black Sea exhibits a cyclonic dominated and time dependent circulation that show strong spatial structure. A Rim Current flows along the perimeter and the continental slope. The interior basin features few major cyclonic gyres. There is also a series of anitcyclonic eddies inshore of the rim current. All these features show strong variability seasonally.

Satellite oceanography has revealed that the Rim Current meanders and that cross stream jets are also dominant features. These jets are common in the summer and autumn and do not exhibit preference for an particular locality [11]. Figure 3-1 shows the bathymetry of the Black Sea. Figure 3-2 gives a schematic of the surface circulation.

3.1   Wind Driven Circulation

The wind driven circulation alone can reveal many of the circulation features that are observed in the Black Sea. Some of the predominant features attributed to the wind driven circulation are the overall cyclonic basin circulation and the meandering Cim
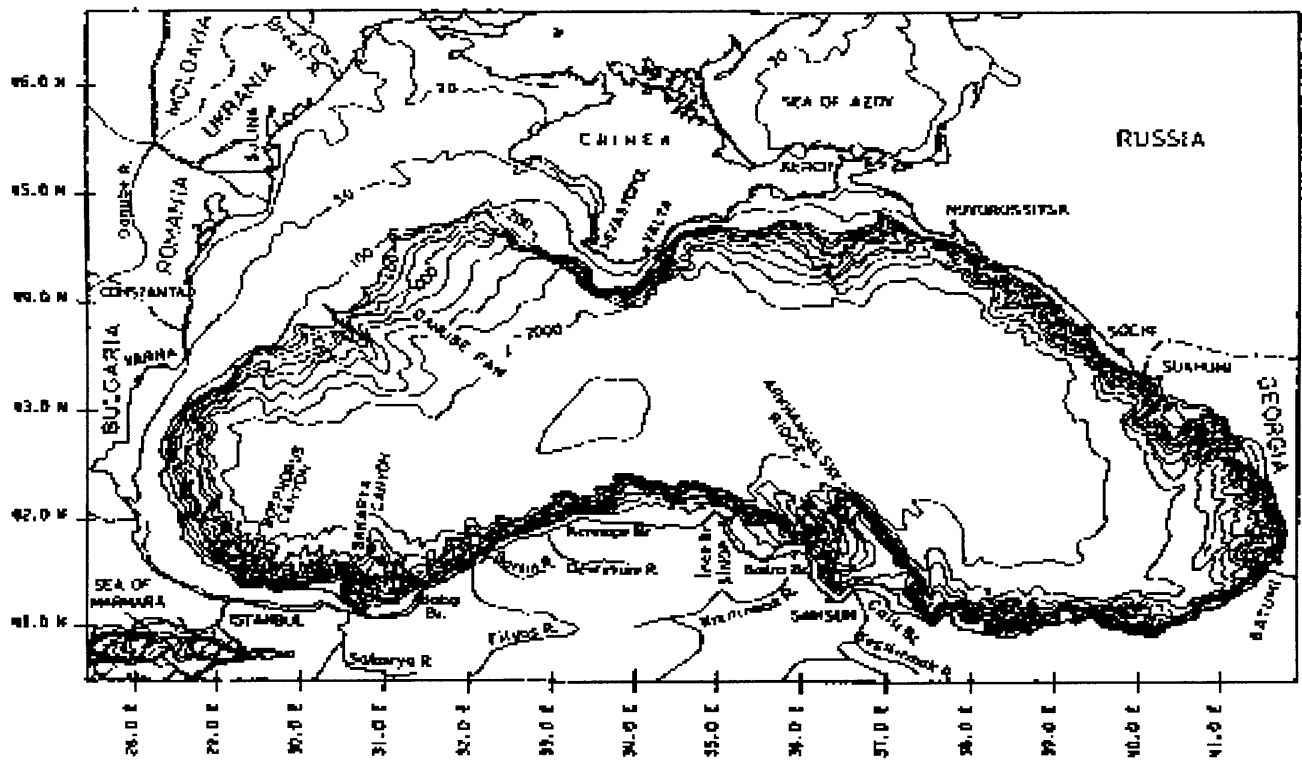
Figure 3-1: This is a bathymetry map of the Black Sea region.
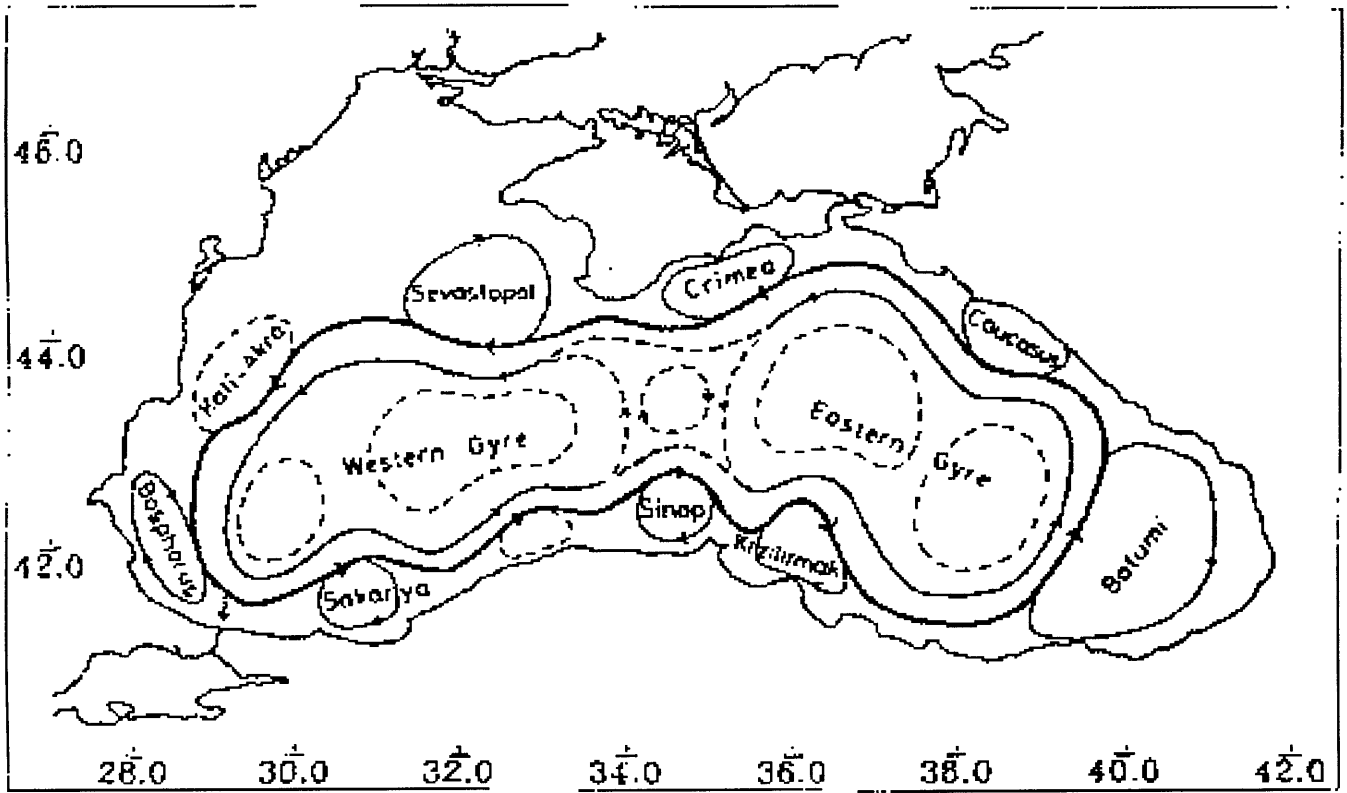
Figure 3-2: A schematic of the Black Sea surface circulation.

Current. These features are additionally reinforced by the influence of river input and by the thermohaline circulation [12].

3.2 Vertical Stability

As mentioned previously, the Black Sea basin is nearly anoxic. Deep waters are rich in hydrogen sulfide and the only upper 150 meters have measurable amount of oxygen. These layers are separated by a permanent halocline. There is also a seasonal thermocline at 15-30 meters depth that affect baroclinic processes [11]. The Black Sea is also very sensitive to changes in its salinity budget. Modeling studies have shown that without the input of fresh river water, the Black Sea loses its vertical stability.

3.3 The Northwestern Shelf

River input affects in the surface circulation in the northwestern shelf. In this area, there are two sources of buoyancy that act opposite to each other. One source is the Danube; the other is the effect of winter cooling. The freshwater source of the Danube and increases vertical stability while winter cooling, by inducing convective mixing, decreases it. Thus the river outflow affects expecially the summer condition characterized by poor ventilation all over the shelf [16].

Freshwater discharge can drive basin-wide cyclonic circulation and an anticyclonic gyre in the northwestern shelf. The freshwater discharge from rivers in the northwestern coast cause substantial variations in the salinity of this region. Around the river mouths, the salinity variations are on the order of 5 parts per thousand.

The summer time temperature of this water is also 2 degrees warmer than the central basin water. Due to its shallow depth, the shelf region in winter is affected by the greatest cooling rate. Changes in river input and temperature correspond to changes in eddy formation and shape of circulation structures in the northwestern shelf. [12].

Chapter 4

Instrumentation and Data

4.1 Remote Sensing

The techniques described in the following sections rely primarily on the use of remotely sensed ocean color. Remote sensing has reshaped the way scientists view the oceans. Only from space can one see the extent of a phytoplankton bloom both spatially and temporally. Ocean color can be measured remotely by studying the amount of light reflected by the ocean surface at a series of wavelengths.

A combination of suspended sediment and chlorophyll cause the oceans to appear colored. Phytoplankton, single cellular aquatic plants, is the main source for the chlorophyll that gives the water a greenish color where they bloom. As seen in Figure 4-1, the quantity of chlorophyll in water can affect the amount of sunlight reflected as a function of wavelength. Generally, phytoplanktonic pigments absorb energy in the red and blue portions of the spectrum, but reflect in the green — giving the water a green tint. Comparing the ratios of the amount of light reflected off the ocean surface at red and blue wavelengths to the amount reflected in the green portion of the spectrum provides a measure of phytoplankton in the water.

To gain a full view of the spatial extent of blooms, data must be acquired remotely. Ocean vessels move too slowly and can only take measurements in a small part of the ocean at any given time. Using satellites to make measurements of ocean color allows for the creation of chlorophyll synoptic maps. Thus phytoplankton can be used as a
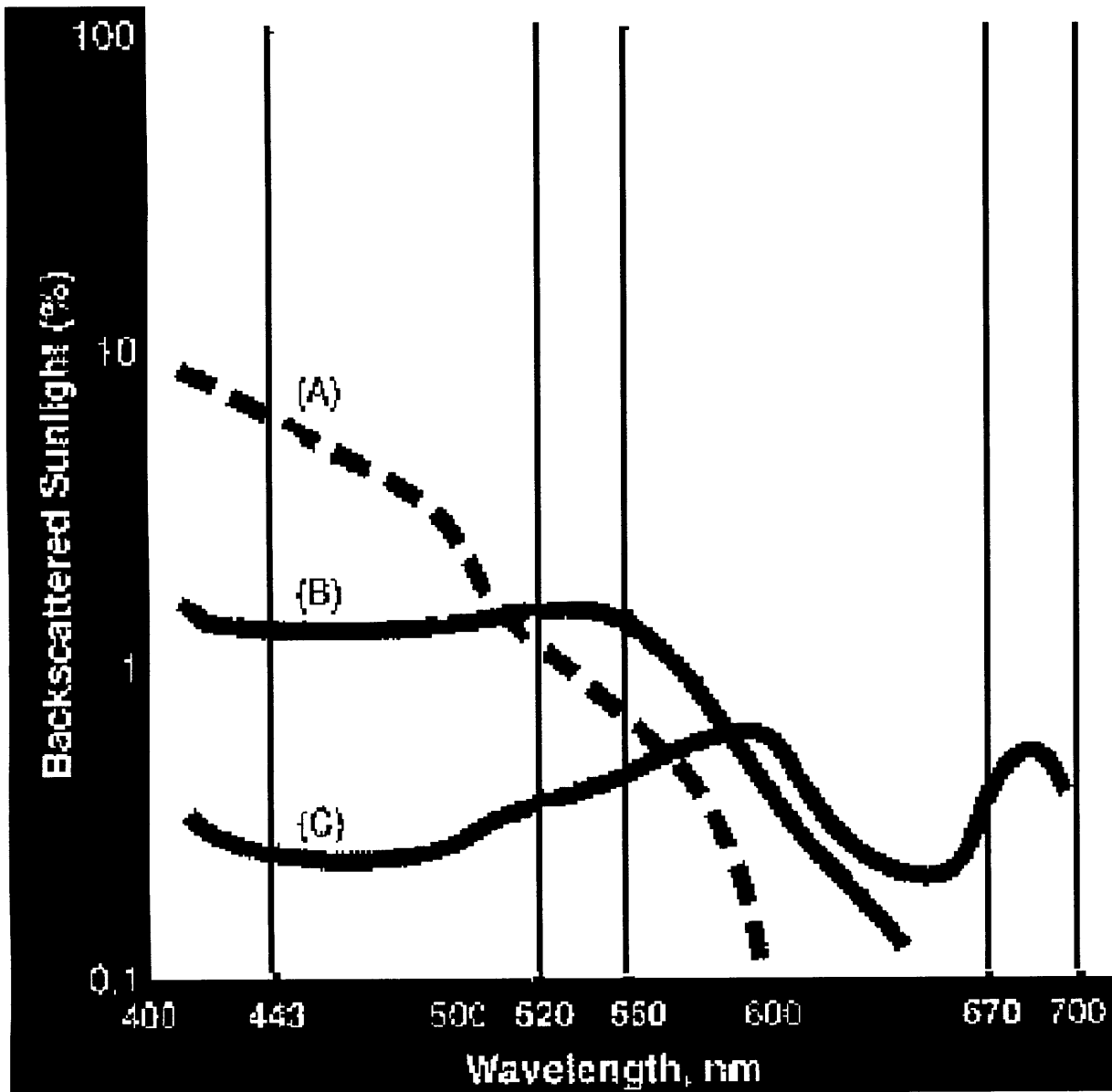
Figure 4-1: This plot shows the percentage of sunlight backscattered from ocean surface as a function of wavelength for several water types. Curve A represents clear ocean water. Curve B is a moderate phytoplankton bloom in the open ocean; Curve C is representative of coastal waters containing sediment well as phytoplankton. The bold lines are representative of measurement wavelengths for the Coastal Zone Color Scanner (CZCS). These bands have been shifted for the SeaWiFS sensor. [10]

tracer of dynamic features. [10]

4.2 Instrument Description

The data used in this thesis was collected by the Sea-viewing Wide Field-of-view Sensor (SeaWiFS) project at the NASA Goddard Space Flight Center (GSFC). This instrument is designed to quantify ocean bio-optical properties. These bio-optical properties are typically caused by phytoplankton since the visible color of the ocean varies with plant pigments such as chlorophyll. As the quantity of plants increases, the water appears greener and will reflect more light at that wavelength. [6]

SeaWiFS is based on the heritage of the Coastal Zone Color Scanner, that was carried on the NASA NIMBUS-7 satellite from 1978 to 1986 as a proof-of-concept instrument. This was the first instrument dedicated to observing ocean color from space and was designed to measure upwelling radiance. Observations made from the CZCS NIMBUS Experiment Team (CZCS-NET) and technology improvements provide the basis for improvements in the SeaWiFS instrument. [1]

The SeaWiFS instrument flies aboard the SeaStar spacecraft. The instruments is an optical scanner with central wavelengths (also referred to as bands) as listed in Table 4.1. The instrument includes an off-axis folded and half-angle mirror that are phase-synchronized. This allows the absence of field-of-view rotation which, in turn, makes the use of a multichannel, time-delay, and integration processing in each band to achieve the necessary signal-to-noise ratio (SNR). An electronics module is also featured. A line drawing of the instrument can be seen in Figure 4-2.

Incoming scene radiation is collected by the folded telescope and reflected to the rotating half angle mirror. Using a beam splitter, this radiation is then divided into four wavelengths intervals that contain the eight SeaWiFS bands. Spectral band-pass filters then separate the radiation into the eight spectral bands. The detected radiation is the amplified and processed in the electronics module [5].
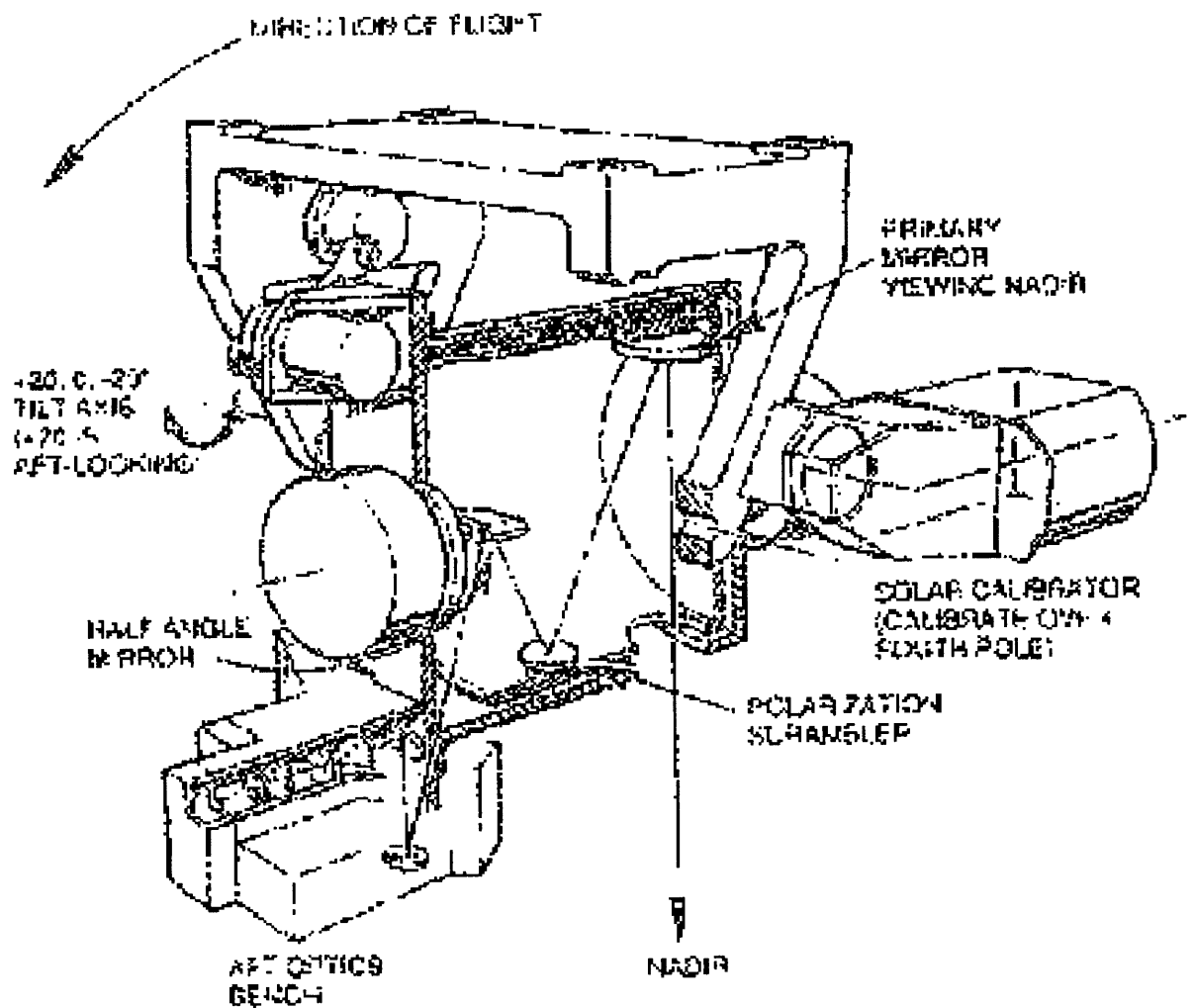
Figure 4-2: This is a labeled line drawing of the SeaWiFS instrument. [5]

4.3 Data Description

Once data is collected on board the SeaStar satellite, it is broadcast directly to a network of ground stations. At this stage, the data is considered to be Level-0 data. It is of one of two resolutions, either local area coverage (LAC) or global area coverage (GAC) data. While LAC data is of higher resolution (1.1Km), this data is collected upon request and has a smaller coverage area and temporal frequency.

Therefore, this thesis relies primarily on GAC data which has an initial resolution of 4.4km at nadir. This dataset is created by preserving every fourth pixel from every fourth scanline. A visualization of this process can be seen in Figure 4-3. Each
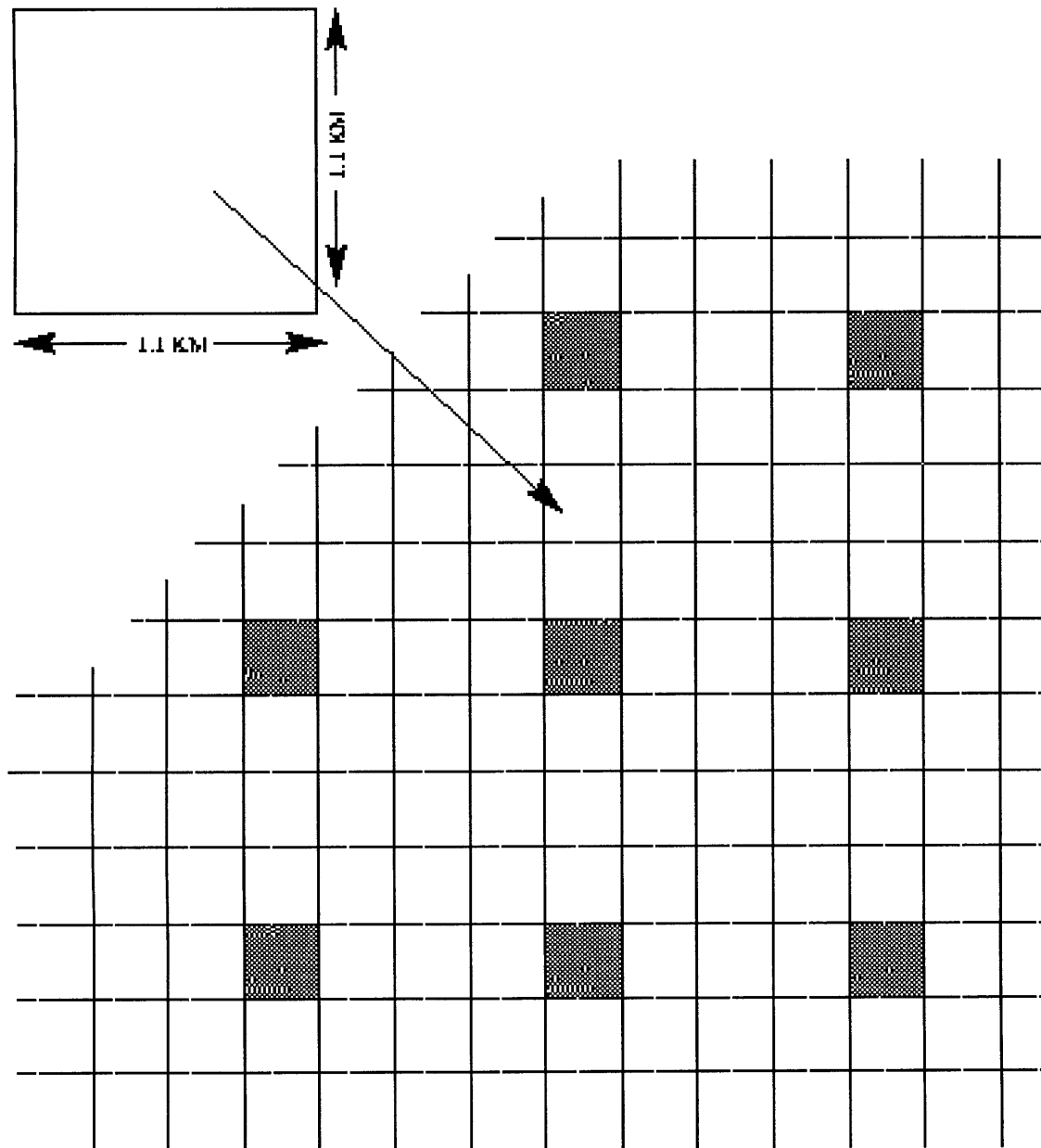
Figure 4-3: This is a depiction of the SeaWiFS GAC sampling algorithm. Every fourth pixel from every fourth scan line is transmitted to create GAC data. Each pixel is also representative of a 1.1X1.1 KM surface.

Band	Wavelength
1	402-422nm
2	433-453nm
3	480-500nm
4	500-520nm
5	545-565nm
6	660-680nm
7	745-785nm
8	845-885nm

Table 4.1: The wavelengths of observation of the SeaWiFS sensor.

preserved pixel is representative of the pixels surrounding it, reducing the resolution. This method reduces the likelihood that data is obscured by clouds or other data obscuring phenomena and will need be present in the final data set. Reducing the number of cloud obscurred data points at this level reduces the likelihood that cloud obscured data will be present in the final data set. This is of concern since cloud detection algorithms are not completely accurate. [2].

The SeaWiFS project offers data to authorized users at several levels of processing. For the purposes of this project, I have chosen to use daily, level-3, binned data. This is the first level of processing that offers spatially and temporally averaged data. While these averaging methods lower the resolution further, there are considerable improvements in data coverage with the statistical processing.

The resulting data products are place into "bins" that are representative of a 9km x 9km area of the Earth's surface. There are 5,940,422 bins stored in each global, Level-3 binned data file. This data is available from the NASA GSFC Earth Sciences Distributed Active Archive Center (DAAC). It is possible to request data to be placed on an file transfer protocol (FTP) server through a web browser interface. SeaWiFS data is available in hierarchical data format (HDF) files.

HDF is a multi-object file format created by the National Center for Supercomputing Applications at the University of Illinois. It allows the storage of many different types of data, including images and multidimensional arrays. While this structure is

complicated, HDF has the advantages of being portable to many different computational platforms and can be used by many programming languages. An example of the HDF structure used by SeaWiFS can be seen in Figure 4-4[8].

In order to simplify the use of SeaWiFS data, the SeaWiFS project group produces a a software package — SeaWiFS Data Analysis System – SeaDAS. This package, however, requires considerable computational power and costly software products. For this reason, MATLAB was used to breakdown the HDF files, isolate the Black Sea region, and store variables of interest from this smaller data set in binary format. A copy of the MATLAB programs used for this purpose is given in Appendix A.

Level 3 binned data includes data from 6 bands in the visible spectrum and 2 outside of it for atmospheric correction. Additionally, these bands of data are combined to create data products such as Chlorophyll A and CZCS pigment. Each of these products and the 6 bands in the visible spectrum were preserved in the stored binary MAT files for archivial purposes. However, further processing was based solely on the chlorophyll product.

This chlorophyll product is meant to be a direct measure of the amount of phytoplankton present in a given area. It is calculated using a ratio of the reflected radiance at 490 nanometers (nm) and 550 nanomenters in the following equations:

$$C = 10^{a_0 + a_1 * R + a_2 * R^2 + a_3 * R^3} \tag{4.1}$$

where

$$a = \begin{bmatrix} 0.450 & -2.860 & 0.996 & -0.3674 \end{bmatrix}$$

and

$$R = log(Rrs_{490}/Rrs_{550}) \tag{4.2}$$

C is the predicted amount of Chlorophyll-A present in the water, and Rrs_{490} and Rrs_{550} are the relected radiances at 490 and 550 nanometeres, respectively. This algorithm is theorized to allow for reasonably accurate results over a large range of
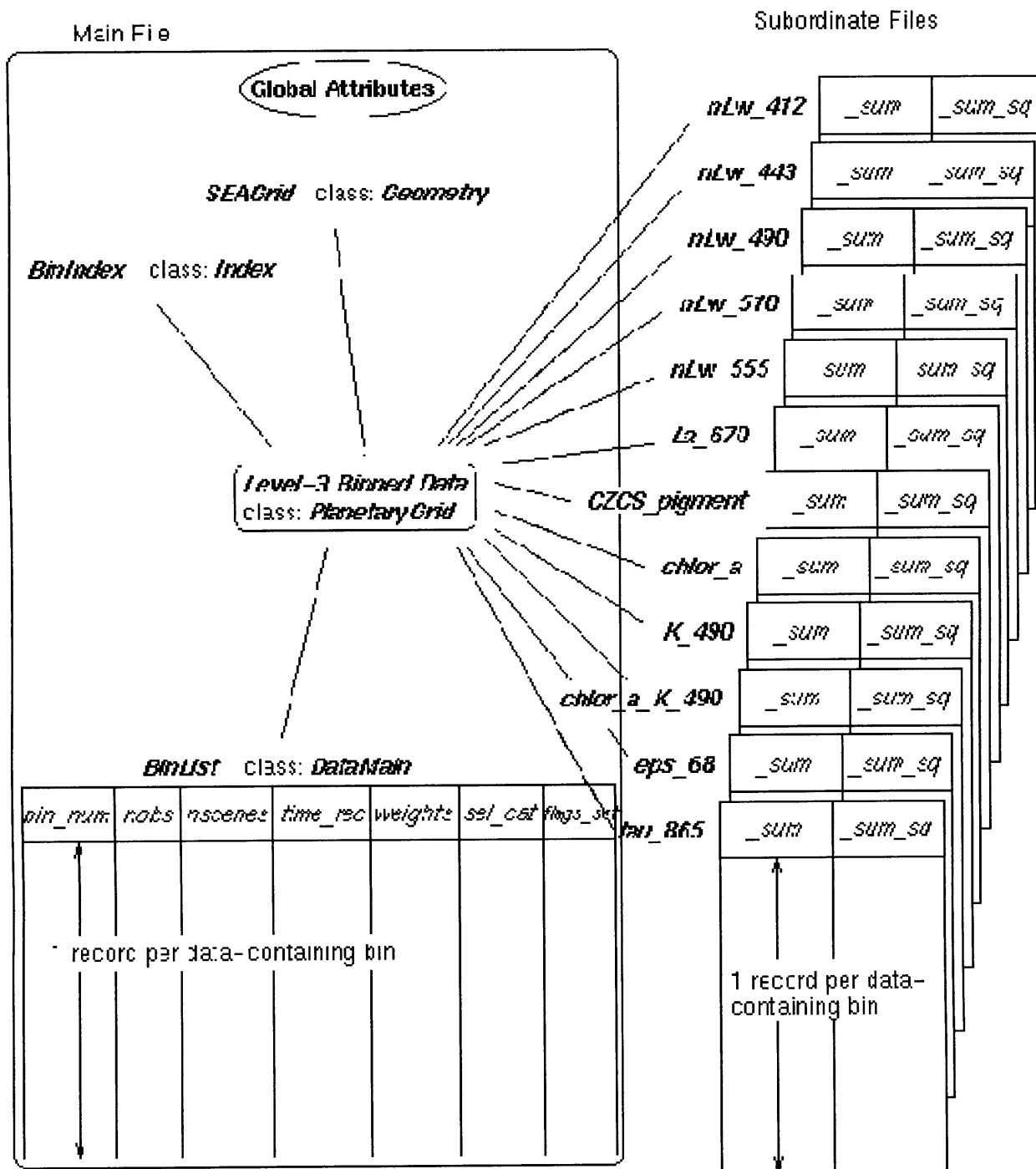
Figure 4-4: A graphical representation of an HDF file structure used to store Level 3, binned SeaWiFS data[4]

Chlorophyll levels and results in a $\frac{mg}{m^3}$ measurement. [13]

4.4 Data concerns

While technology and algorithms improvements during the twenty year period be-
tween the launches of CZCS and SeaWiFS were substantial, there are still concerns
about the usability of this data set for inland seas such as the Black Sea; these wa-
ters are often referred to as case 2. The optical variations in case 2 water is caused
by phytoplankton, inorganic suspended matter and colored dissolved organic matter
(CDOM).[15]

SeaWiFS was designed for the study of ocean color in case 1 waters where the
color variations are caused primarily by changes in phytoplankton blooms. However,
the technology and resolution improvements make it a desirable way to study water
quality in areas such as the Black Sea.

The main limiting factor to this application is the large source of error caused by
the atmospheric correction performed on SeaWiFS data sets. The driving principle
behind atmospheric correction algorithms is that there is no water leaving radiance
in the near infrared part of the spectrum. While this is relatively successful for
reasonably clear water, in highly turbid water or case 2 water this assumption breaks
down.

There are many other suspicious data abnormalities in the Black Sea data sets
that can be attributed to the problem of turbid water and to the general problem
of electronic noise. Contour maps created from the unprocessed show an unusual
amount of variation in abnormal patterns for phytoplankton as seen in Figure 4-5.
There is also some concern about abnormally high values of chlorophyll in some data.
This is attributed to a combined effect of the turbidity of the water and atmospheric
correction problems.
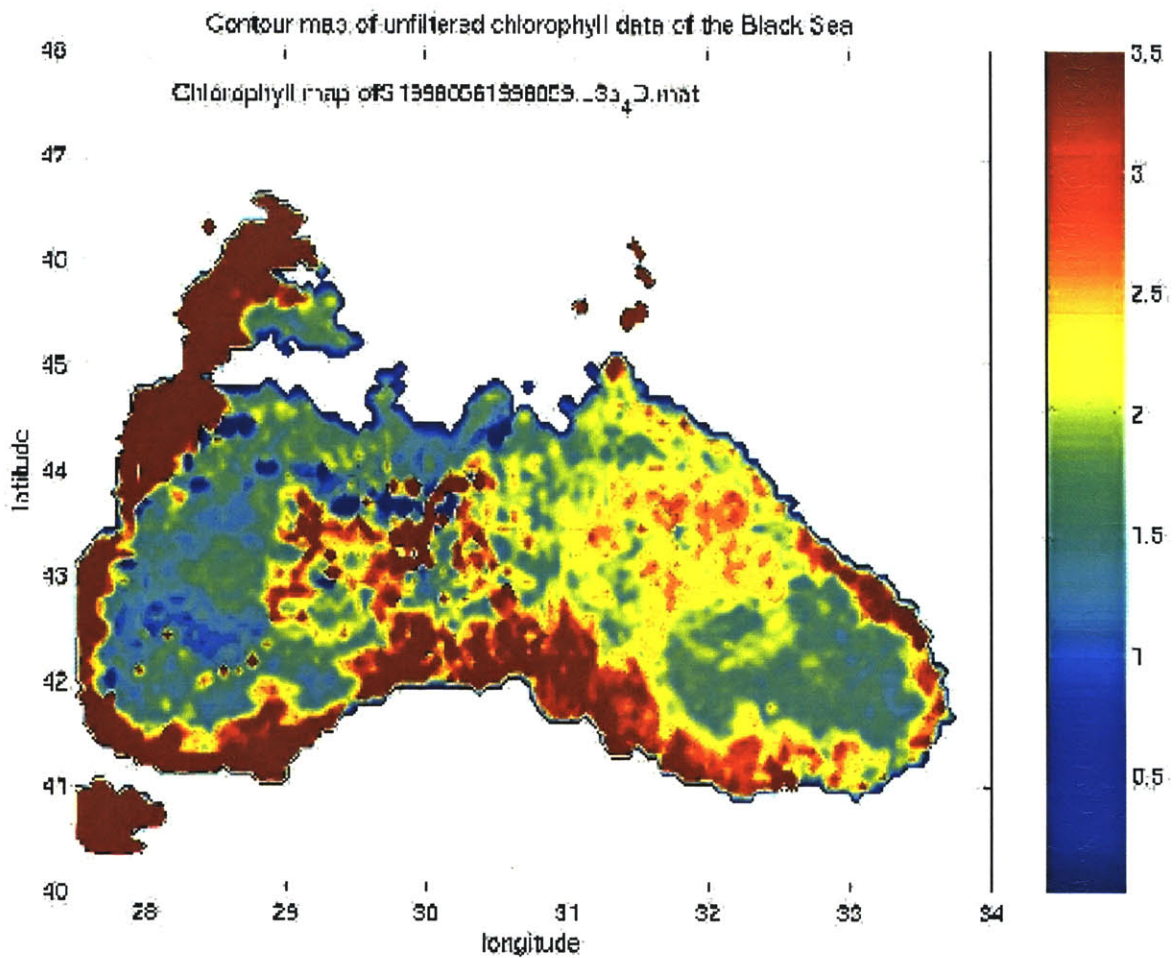
Figure 4-5: As seen in this countour map of 4 day averaged SeaWiFS data of the Black Sea, there is considerable graininess in the image that is unlikely to be caused by data from phytoplankton. One of the suspected causes is electronic noise.

Chapter 5

Methods

5.1   Four Day Averages

One of the big problems with utilizing SeaWiFS data over the Black Sea is a lack of coverage. A combination of the heavy aerosols over the region, poor data quality and a shortage of data collection stations in the region lead to many spatial and temporal data gaps. While different interpolation schemes may help resolve some of these issues, another approach is temporal averaging of data.

While the SeaWiFS group does produce 8 day averaged products, this corresponds to the life cycle of algae. Therefore, it is not appropriate to study the change and movement of many blooms. Also, these 8 day averages are successive rather than running, which reduces the amount of data available.

After spatially selecting the western Black Sea from level 3 binned data files, chlorophyll measurements were averaged for four consecutive days. A four day running average data set was created. On days where data was available for a given location, that data value was included in the average. If no data was available for a location on any of the four days, the data value was left empty. This strategy filled many of the data gaps to make the application of edge detection to the data sets more feasible.

5.2 Edge Detection and Noise Suppression

There is considerable interest in being able to identify circulation features automatically. While there are many ways to approach this problem, edge detection is an elegant solution to it. Also, many methods of edge detection have the additional advantage of being image processing techniques that can be applied independent of the data set.

The application of edge detection is an attempt to find regions of change in a two dimensional data set or image. In oceanography, these regions correspond to underlying oceanographic and biological phenomena, such as the formation of phytoplankton blooms, eddies, currents, or regions of convergence. Edges have been found manually for years in an effort to find these features of interest.

As computational facilities improve and as remote sensing data becomes more prominent, there is increasing interest in being able to automate this process. An automated system allows for the standardization of change analysis. Furthermore, analyzing change analysis computationally allows for ready statistical analysis to distinguish between false and present circulation features.

Since the field of edge analysis is an image processing technique, there has been considerable research done on improving algorithms and filters. Unfortunately, most applications of edge detection are in fields such as machine vision rather than oceanography. This adds additional complexity to the methods of edge detection when used on remotely sensed ocean color data.

5.2.1 Noise

The ocean environment and remote sensing considerations create data sets with a considerable amount of noise. Edge detection algorithms are generally designed to work on low or white noise environments, with typical applications such as optical character recognition and machine vision.[3]

Furthermore, most edge detection algorithms seek out gradients. These gradients are typically found in the high frequency regions of the image. Most edge detecting

filters are simply some variety of high pass filter. Unfortunately, most oceanographic noise is also considered high frequency. As a result, the edge detecting filters extract both the change features as well as noise. This increases the likelihood of false feature being detected.

For this reason, care must be taken to suppress the maximum amount of noise from a data set before applying any filtering techniques. There are many approaches to to this. One is to apply a low pass filter to the data set. The problem with such an approach is that areas of change are high frequency features. While a low pass filter would in fact remove a good deal of white noise from an image, it would also decrease the features of interest.

Another possible solution is to apply thresholding to a dataset. The SeaWiFS data set, particularly around inland seas and coastal regions, often includes data values that are unreasonably high. The accuracy of these measurements is poor and the abnormally high values often cause the determination of false edges. It is, however, likely that the amount of chlorophyll associated with these false highs is considerably large.

Using this assumption, some noise reduction may be performed by thresholding an image such that there is a saturation and cutoff value associated with it. For instance an given map has a maximum chlorophyll value of $4\ mg/m^3$. Any data values higher than than this are diminished to the maximum value. A similar procedure is performed on low data values as well. The exact amount of chlorophyll is not needed to perform edge analysis since edge detection is based on the difference between adjacent chlorophyll values.

Another approach to noise reduction involves adaptive filtering. Adaptive filters are statistically based. Where the variance in an image window is small, the filter does more smoothing. In areas of larger variance, the filter performs less smoothing. Adaptive filtering often performs better noise reduction than linear filtering. Furthermore, being an adaptive method, it is much better at preserving high frequency information, such as edges. A comparison of all these method can be seen in Figure 5-1.
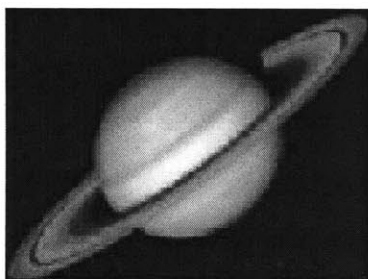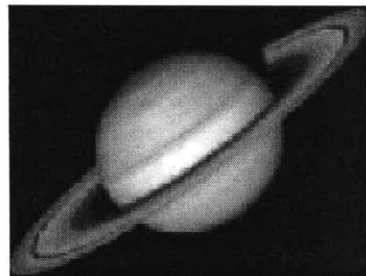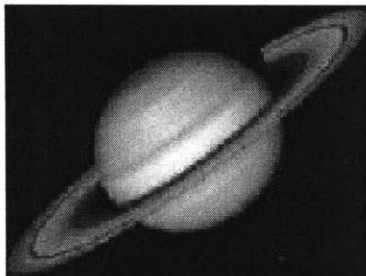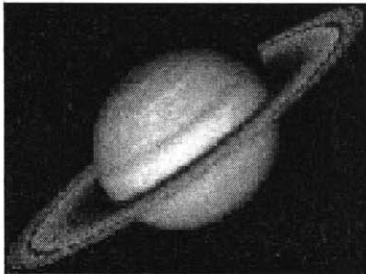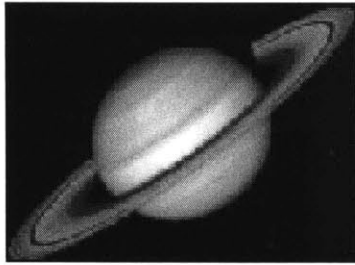
Figure 5-1: These images were produced using MATLAB to demonstrate the effectiveness of different filtering techniques. The top image is the original image of Saturn, the second had Gaussian noise added to it. The remaining images had the following filter applied to them, Wiener filter, Median Filter, Wiener Filter and median filter in succession.

38

5.3 Noise reduction and Edge Detection procedure

The best option for noise reduction and edge detection is the design of a processing bank which utilizes the best of all of the methods. This was the approach taken to edge detect images of the Black Sea.

An unfiltered example map can be seen in Figure 5-2. The amount of texture and variance in chlorophyll measurements in this map makes it impossible to be edge detected. Rather than finding large patterns, the algorithm finds small pockets of slight variation that are more likely representative of noise rather than true variations in data.

A Wiener filtered example can be seen in Figure 5-3. This filter eliminates the speckle noise that makes edge detection difficult on SeaWiFS chlorophyll maps. This adaptive filter also preserves strong edges by allowing the amount of smoothing to vary with the statistical properties of the data in any given pixel windows. The downside to this technique is that the edges remain jagged. Also, there are still residues of noise in the image.

This problem can resolved by following the Wiener filtering process with a Median filter. While the Median filter will soften the edges, maintaining a small window size for the filter will prevent the loss and distortion of gradient information. Applying the Wiener filter before the Median filter allows for a smaller window size and hence improves the accuracy of edge information. The results of applying this filter can be seen in Figure 5-4

Following this step, thresholding is applied to the data set. This prevents the edge detection algorithm from locating variation among very high or very low data values. For our purposes, we are primarily interested in the larger data gradients. However, false highs and lows in data values can mimic these edge points. The data set is thresholded for data values greater than 3.3 mg/m^3 and below 1.2 mg/m^3

To simplify the edge detection process and improve its accuracy, the high frequency information is now accentuated with a high pass filter. This is constructed by subtracting the effects of running a low pass filter (Median filter) over a noise

39
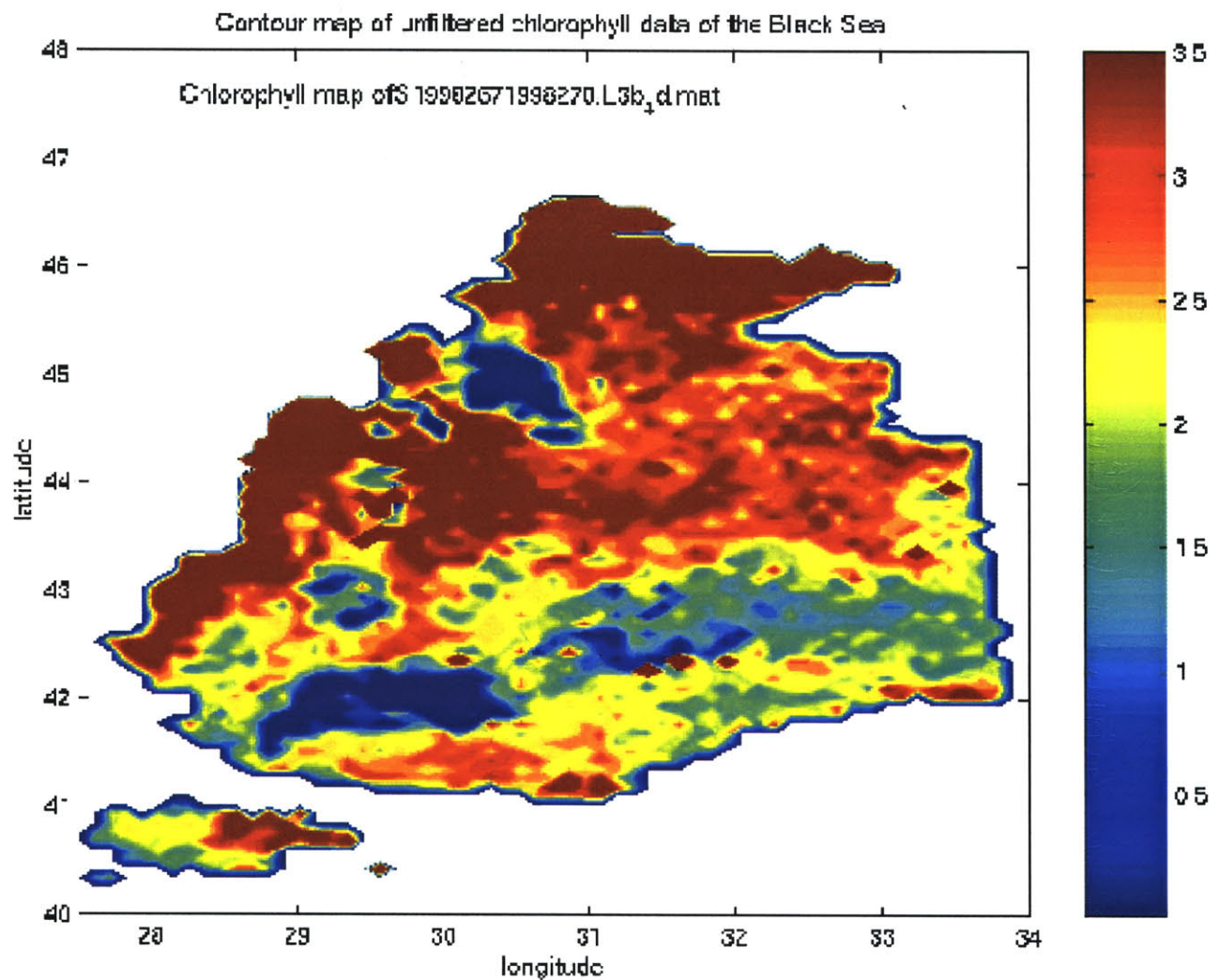
Figure 5-2: This map was created using SeaWiFS Level 3 Binned Chlorophyll product four separate days that were used to create a four day average product. This map is not processed. The amount of texture in the map makes it difficult to be edge detected..
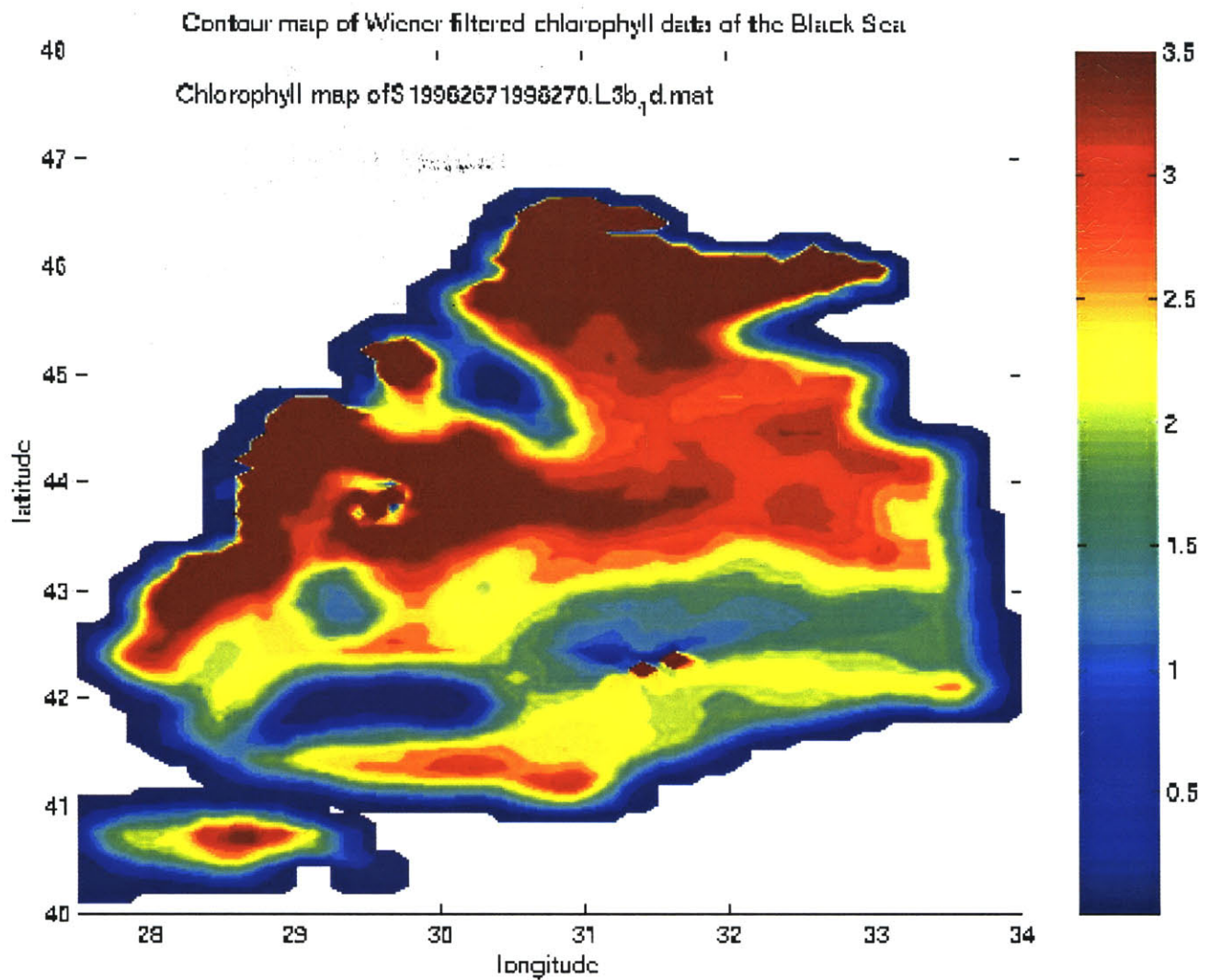
Figure 5-3: This is a chlorophyll map from the same data set that created the map in Figure 5-2 after being Wiener filtered. The Wiener filter smoothes our the data, while preserving high frequency information, such as edges.
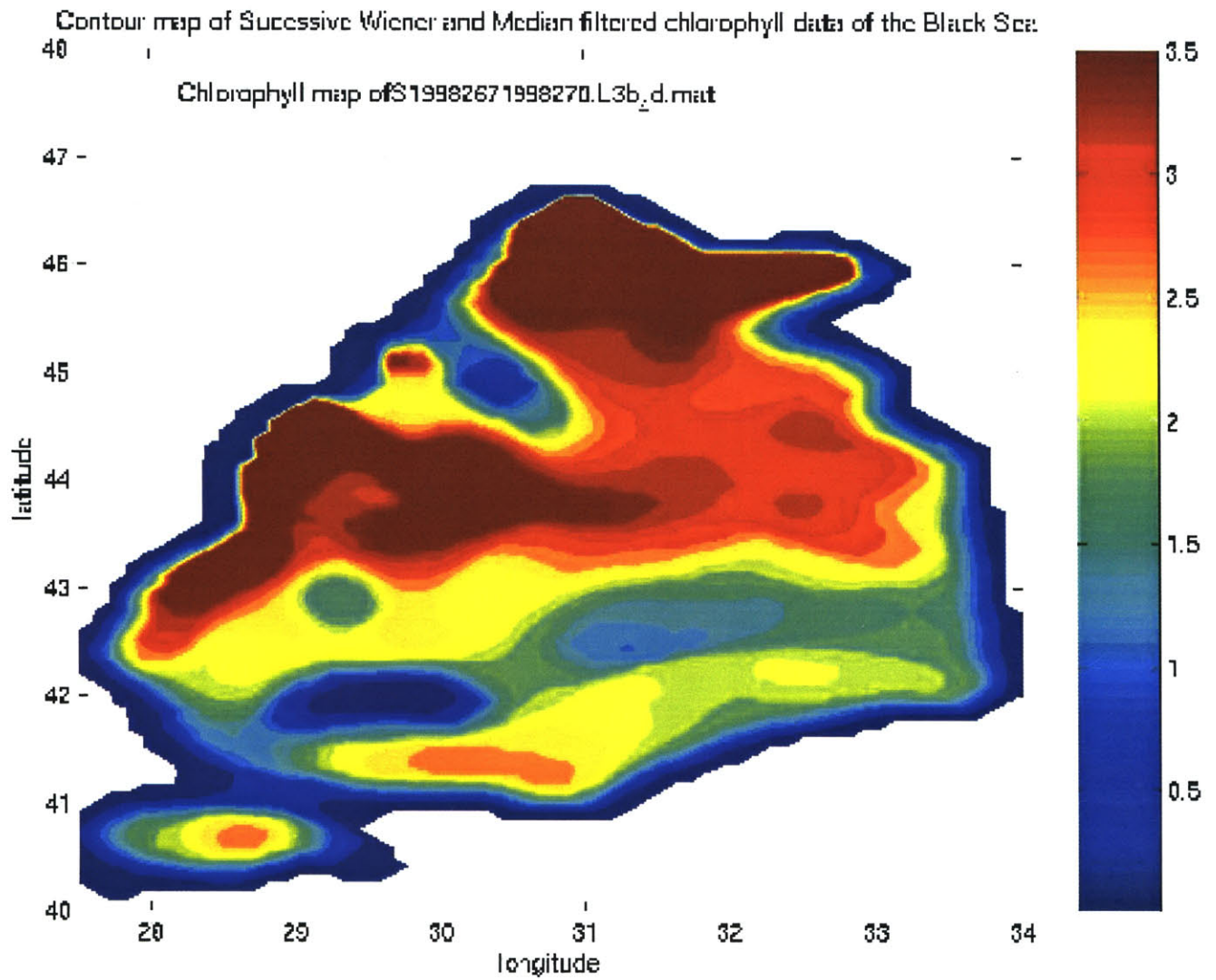
Figure 5-4: This is an example of a chlorophyll map after median filtering the Wiener filtered data shown in Figure 5-3.

reduced data set (Wiener filtered) from the noise reduced data set. High frequency information is the added back into smoothed, noise reduced data set. This makes the edges more prominent and easier to detect using gradients.

In order to detect gradients, the Sobel Edge detector is used. Compared with other edge detection techniques, such as wavelets, the Sobel edge detector is not accurate in noisy environments. However, the simplicity of this method is desirable and Sobel edge detector is the most prevalent scheme in edge detection [7]. This problem has been handled by filtering the data set for noise reduction.

The gradients found using the Sobel edge detector were then thresholded in order to find the appropriate gradient values that corresponded to features that we were attempting to detect. These edges were then superimposed on to a Wiener filtered chlorophyll map to evaluate their effectiveness. A flowchart of this process can get found in Figure 5-5. A full listing of processing code can be found in Appendix B.
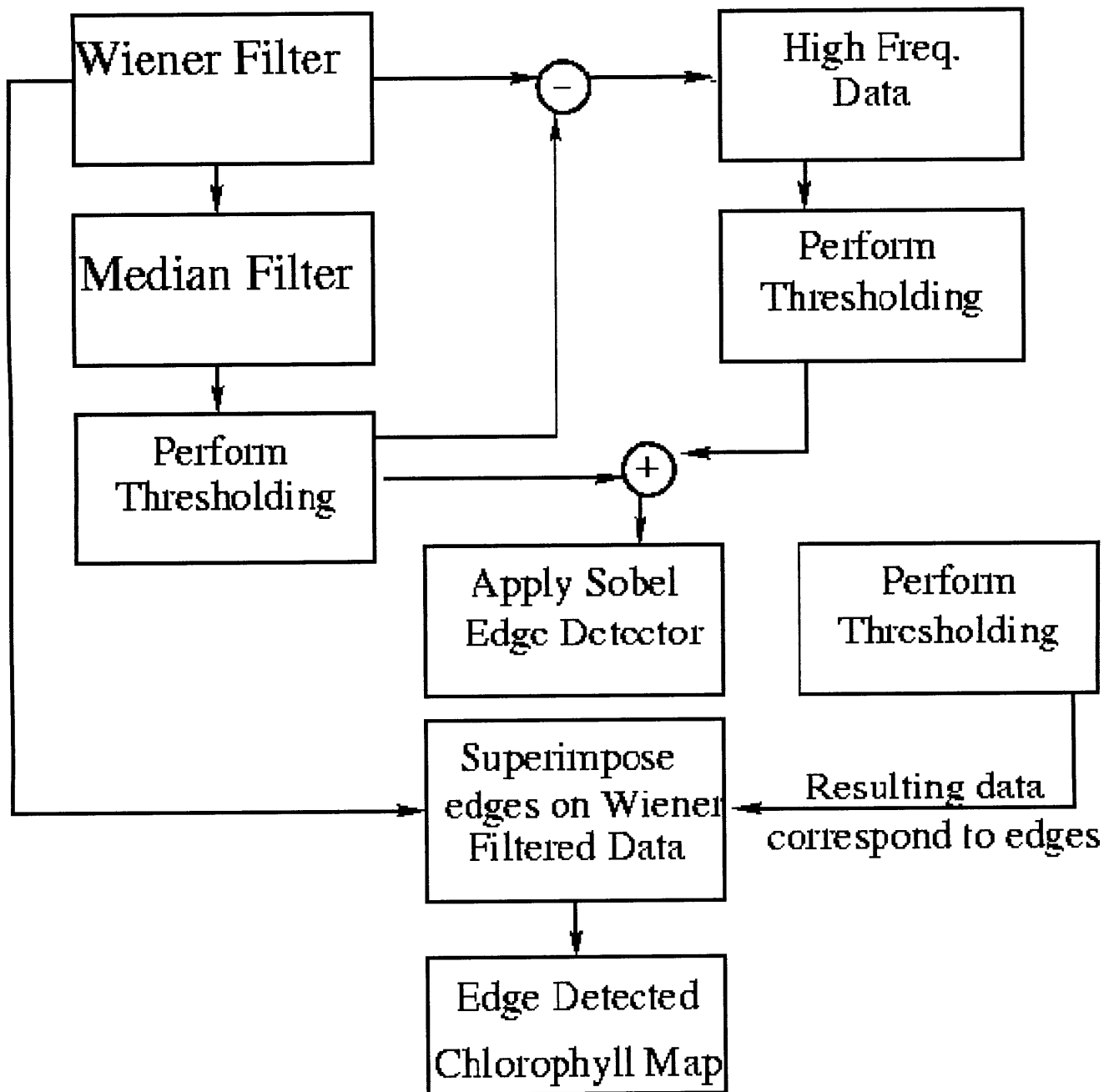
Figure 5-5: A flowchart of the processing algorithm developed for edge detection.

Chapter 6

Results

6.1   Edge Detection Algorithm

The developed edge detection algorithm successfully identifies a water mass in the northwestern shelf that is associated with high nutrient water input from the Danube River. The perimeter of this water mass is identified automatically in the accompanying chlorophyll maps, the detected edge is shown in black. An example is shown in Figure 6-1

A secondary edge is also identifiable in these images . Often, in the lower chlorophyll regions in the maps, a series of red dots can be found along the perimeter of a moderate chlorophyll region. These can also be observed in the maps in Figure 6-1.If connected, these dots identify a weak gradient that is associated with a moderate chlorophyll water mass having moderate chlorophyll content.

Most other studies involving edge detection in oceanography have focused on regions such as the Gulf Stream. Also, they tend to utilize sea surface temperature rather than chlorophyll. For this reason, it is difficult to compare the successfulness of this algorithm with other oceanographic edge detection attempts.

It should be noted however, that this algorithm does tend to identify as many edges as are seen in the studies that utilized sea surface temperature data. This may be in part due to the different nature of variance in Sea Surface Temperature. The edge detection algorithm designed for this thesis also limits the number of edges found
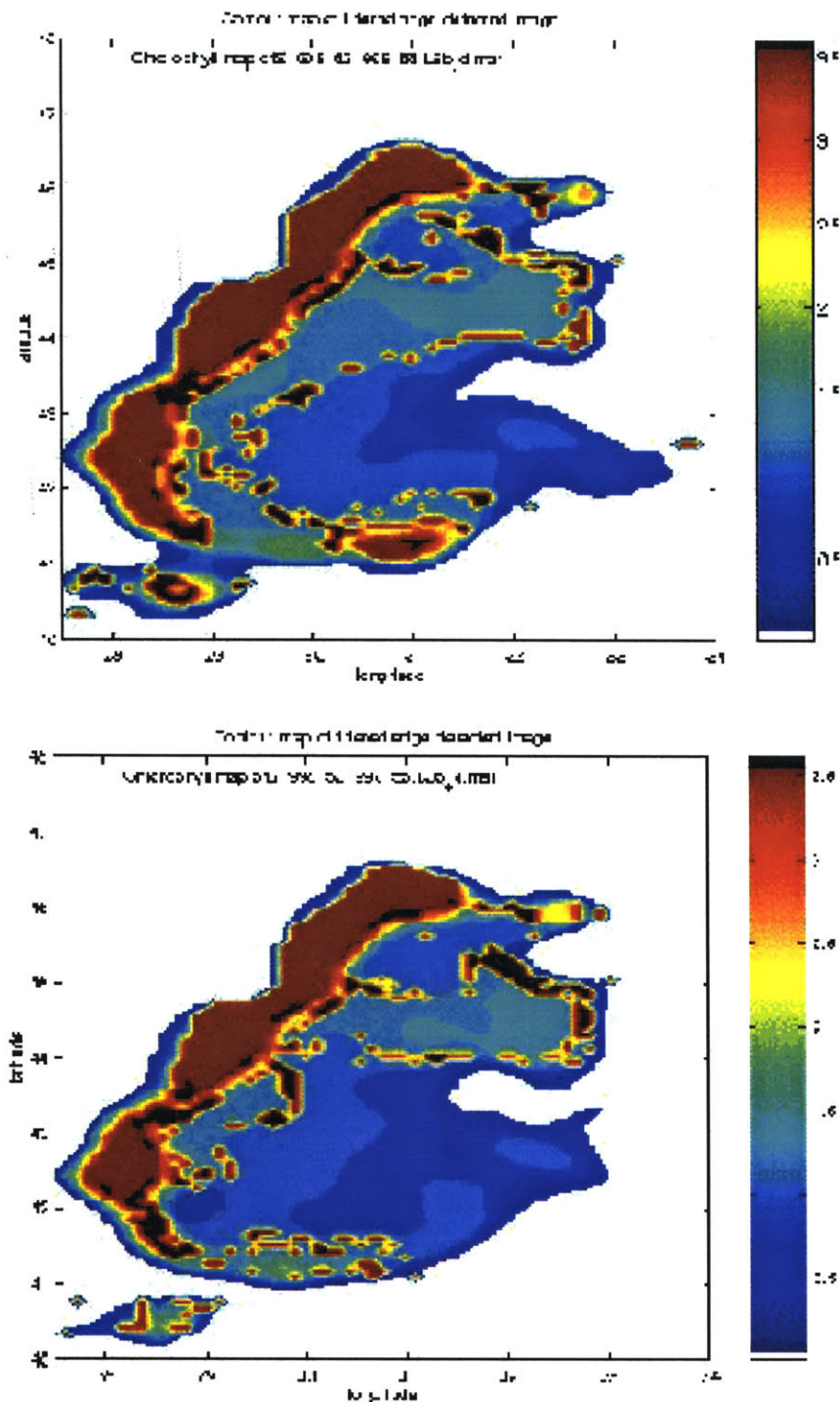
Figure 6-1: These two maps were creating using 4 day averaged data collected between days 152 and 156 in 1998 (early June). The black lines around the perimeter of the high chlorophyll region is a detected Edge. A secondary edge can be seen and is identified by the red dots among moderate chlorophyll regions. It is also notable that during this time period, the high chlorophyll region extends along the western coastline of the Black Sea.

in order to simplify the analysis and limits the effects of noise in the edge-detected maps.

6.1.1 Failure Scenarios

The edge detection is not universally successful. While it works well in most cases, there are several examples in which the algorithm is failure. These failure examples are easily understood, however, by examining the edge detection algorithm.

One of the problems with the described algorithm is that it is structured to avoid detecting high gradients. This feature helps to avoid the detection of noise as a front. Unfortunately, in maps where fronts appear as genuine step functions, these fronts cannot be identified. This particularly becomes a problem during the autumn when the western Black Sea is in full bloom (Figure 6-2).

Another concern about the edge detection algorithm is the fact that the detected edges obscure data values. These data values can provide important information about the characteristics of regions of change. In many cases this is not a strong concern; however, in some images the detected edges are rather thick, often several pixels wide.

6.2 Scientific Results

During the summer of 1998, many interesting oceanographic features can be observed in remotely sensed ocean color maps. In the northwestern shelf, the high chlorophyll region can be attributed to the nutrient rich water of the Danube. The motion, shape, and changes in this high chlorophyll region is studied here.

During early June of 1998, the water mass extends north to south along the western coast (Figure 6-3). As mid-June is approached, a break forms in the middle of the high chlorophyll mass. It can be seen in Figure 6-4, bottom panel. The northern and southern masses then rejoin a few days later and remain reasonably stationary until late June. At this time the water mass begins to move northward. By the end of the month, the high chlorophyll region is located in the northwestern part of the
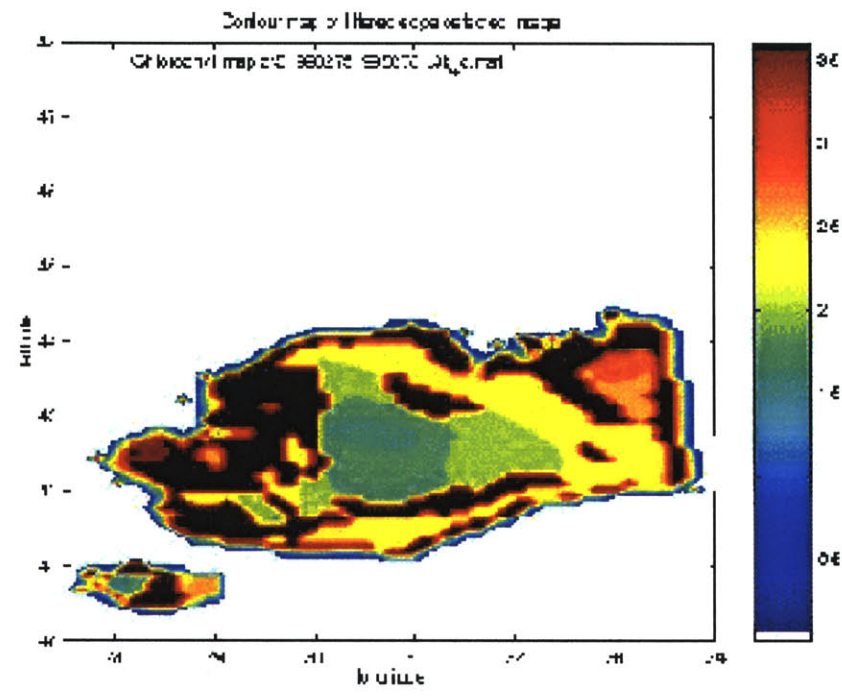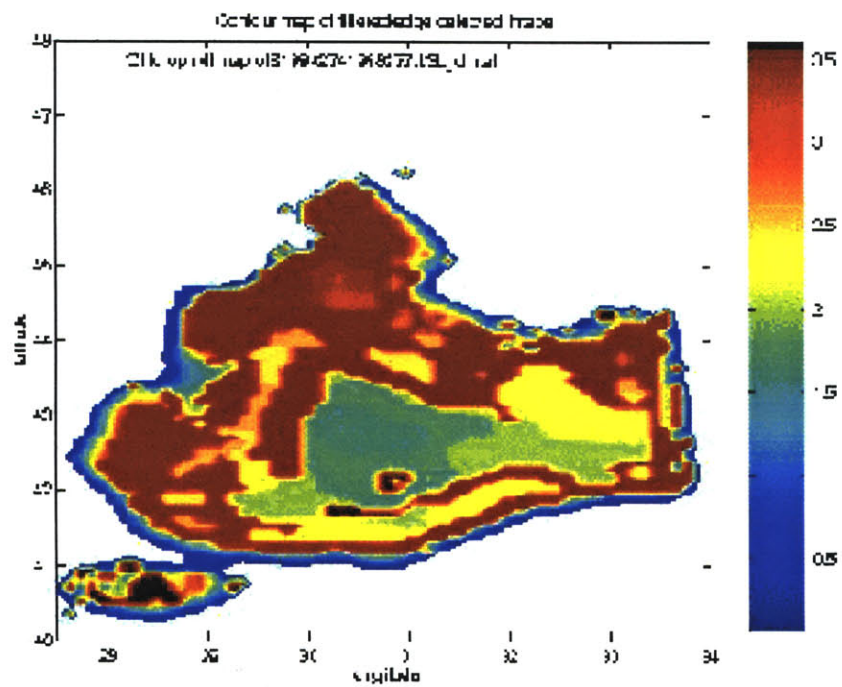
Figure 6-2: During Late September to Mid October, the western Black Sea features large blooms. This causes a failure of the edge detection algorithm.
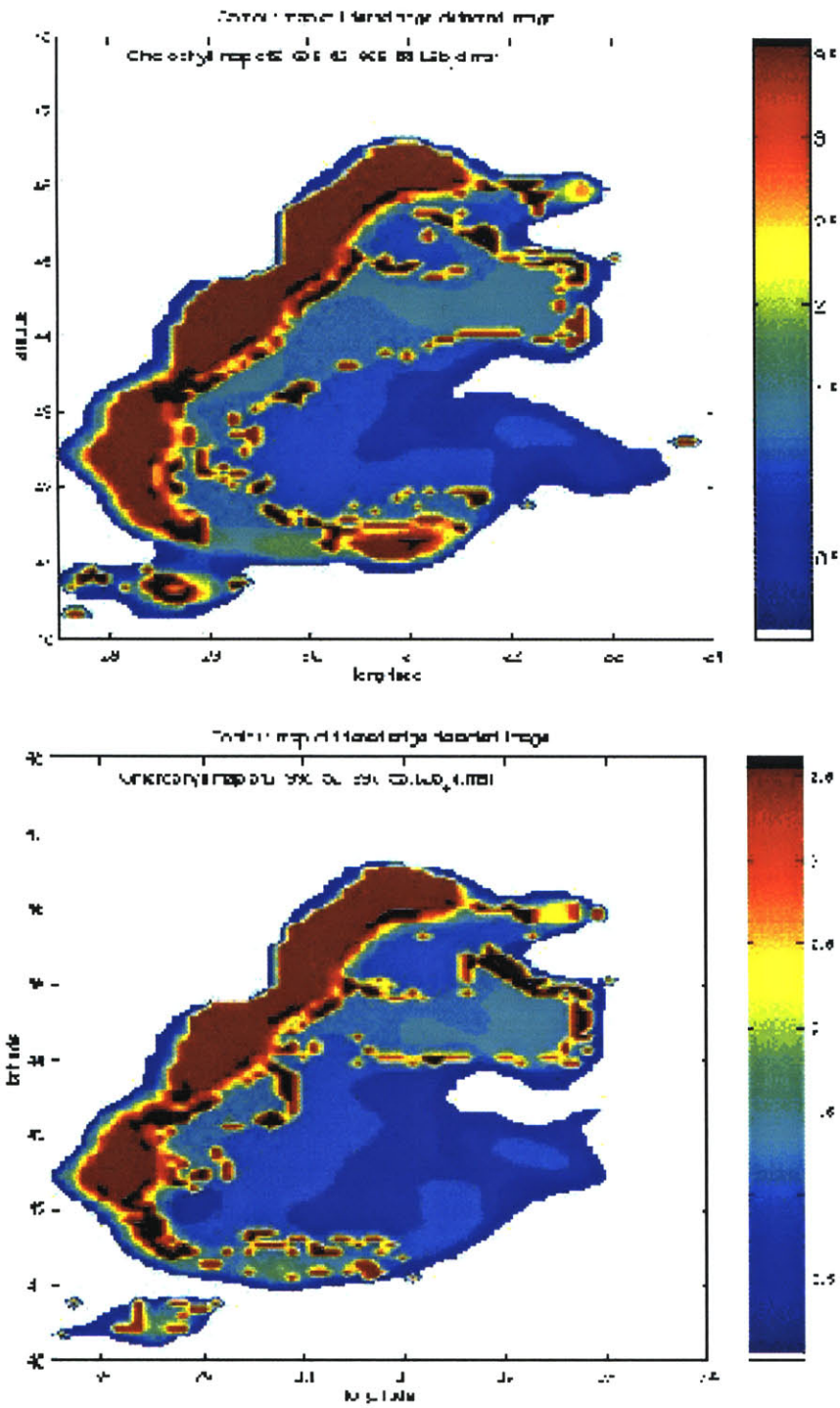
Figure 6-3: Chlorophyll maps from early June.
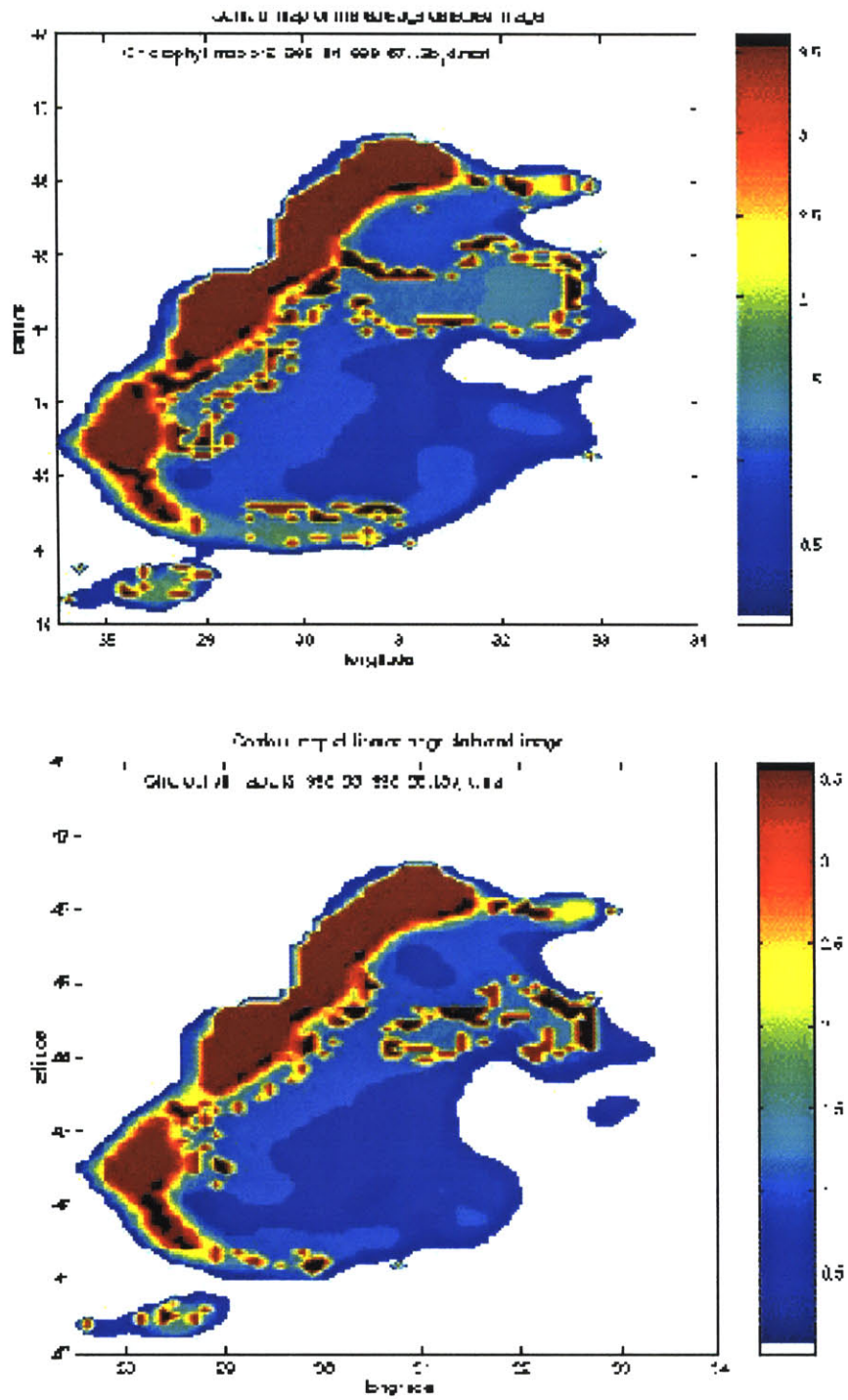
Figure 6-4: Chlorophyll maps from early June.
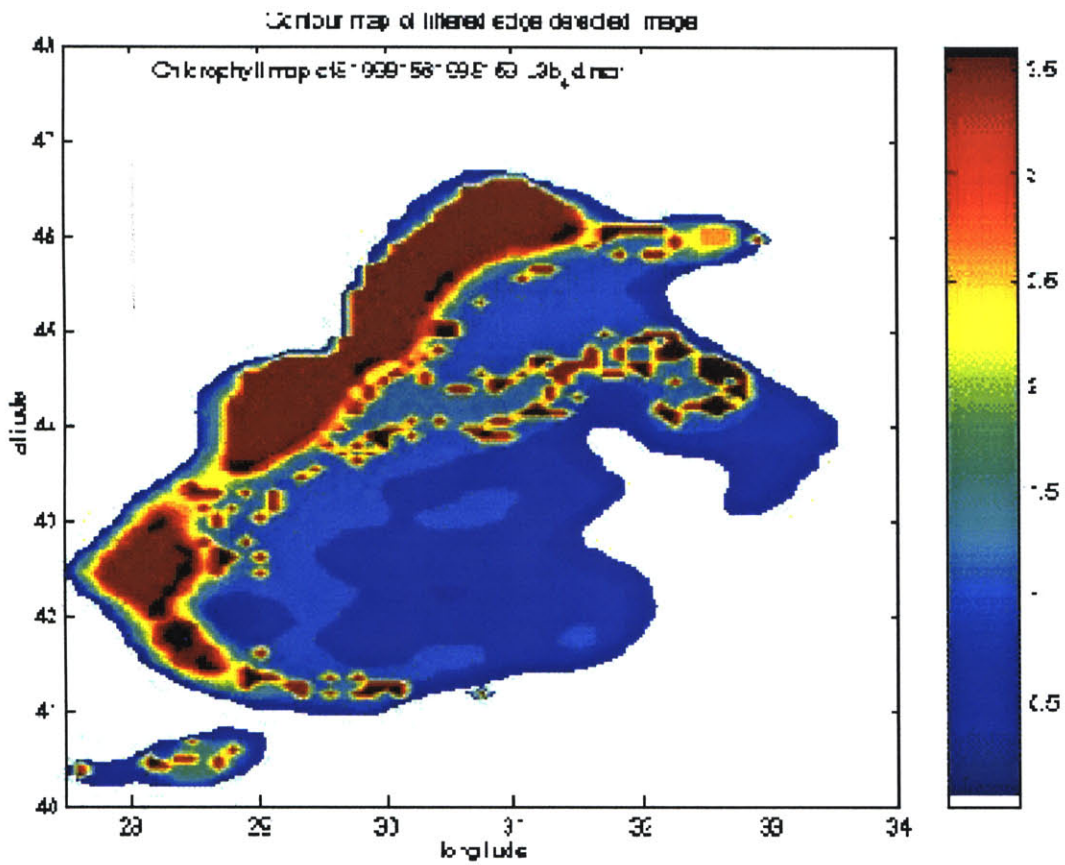
Figure 6-5: Chlorophyll maps from early June.

Sea (Figure 6-6).

In July, the high chlorophyll water is still in the northwestern sea (Figure /ref-fig:july2). However, portions of the water mass begin to extend out towards the southwestern basin. Beginning on day 185 (Figure 6-7), a secondary edge outlines a finger-like moderate chlorophyll region extending out towards the center of the Black Sea shelf from the high chlorophyll water in the northwest and is fully developed by day 189 Figure 6-9. The feature finally disappears two days later (Figure 6-10, bottom panel).

During this time period, the high chlorophyll region also become more restricted to the northern most part of the shelf. The water mass, however, also begins to drift eastward. As the month wears on, the nutrient rich water begins to extend away from the coast.

In August, the water mass starts to drift southward along the coast again. It, however, does remain restricted to the northwestern region. In early September, the chlorophyll region is at a low (Figure 6-11 through Figure 6-14). The high chlorophyll region begins to be to move back towards the northern coast. During the middle of the month, the high chlorophyll region expands dramatically (Figure 6-15 through Figure 6-17).

In addition to the expanding high chlorophyll region, the moderate chlorophyll region also expands during this time. In fact, by day 252, high and moderate chlorophyll regions essentially dominate the entire western shelf. By mid-October, the gradients between high and moderate chlorophyll are so sharp that edges become undetectable.

These results correspond to what models predict will be observed during this time period. The movement of the high chlorophyll region northwards is likely due to the forcing of the Danube. During this time period, its flow increases dramatically. Changes in this flow and it's effect on the salt budget of the Black Sea, keep the high nutrient water in the northwestern portion of the sea. These circulation features can also be seen in model studies [12].
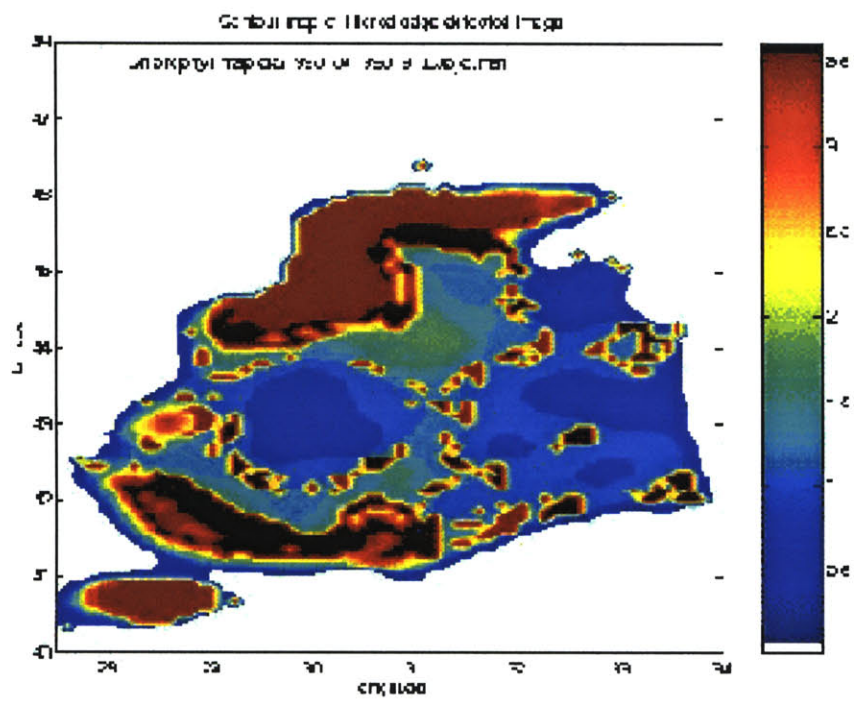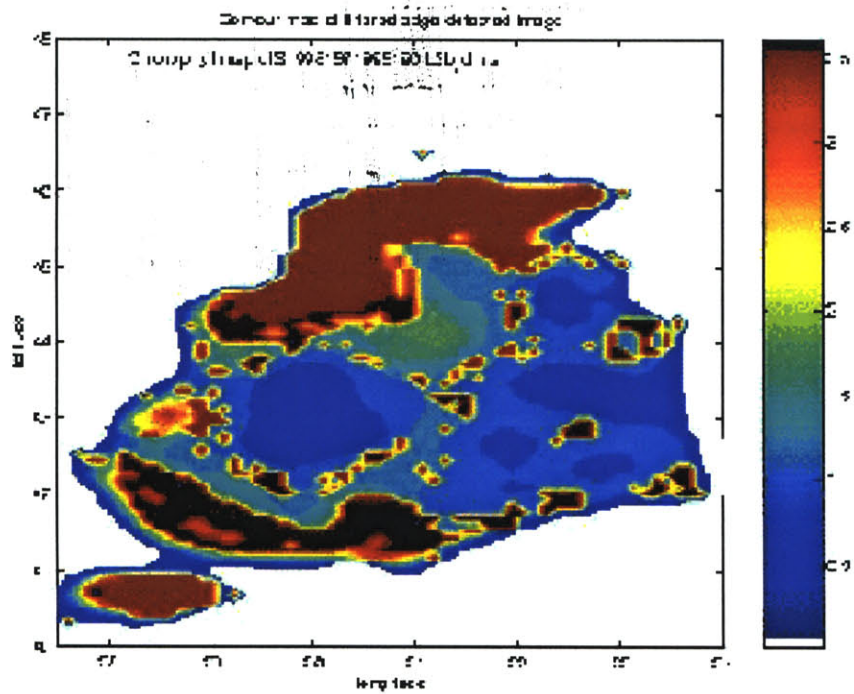
Figure 6-6: Chlorophyll maps from July 1998.
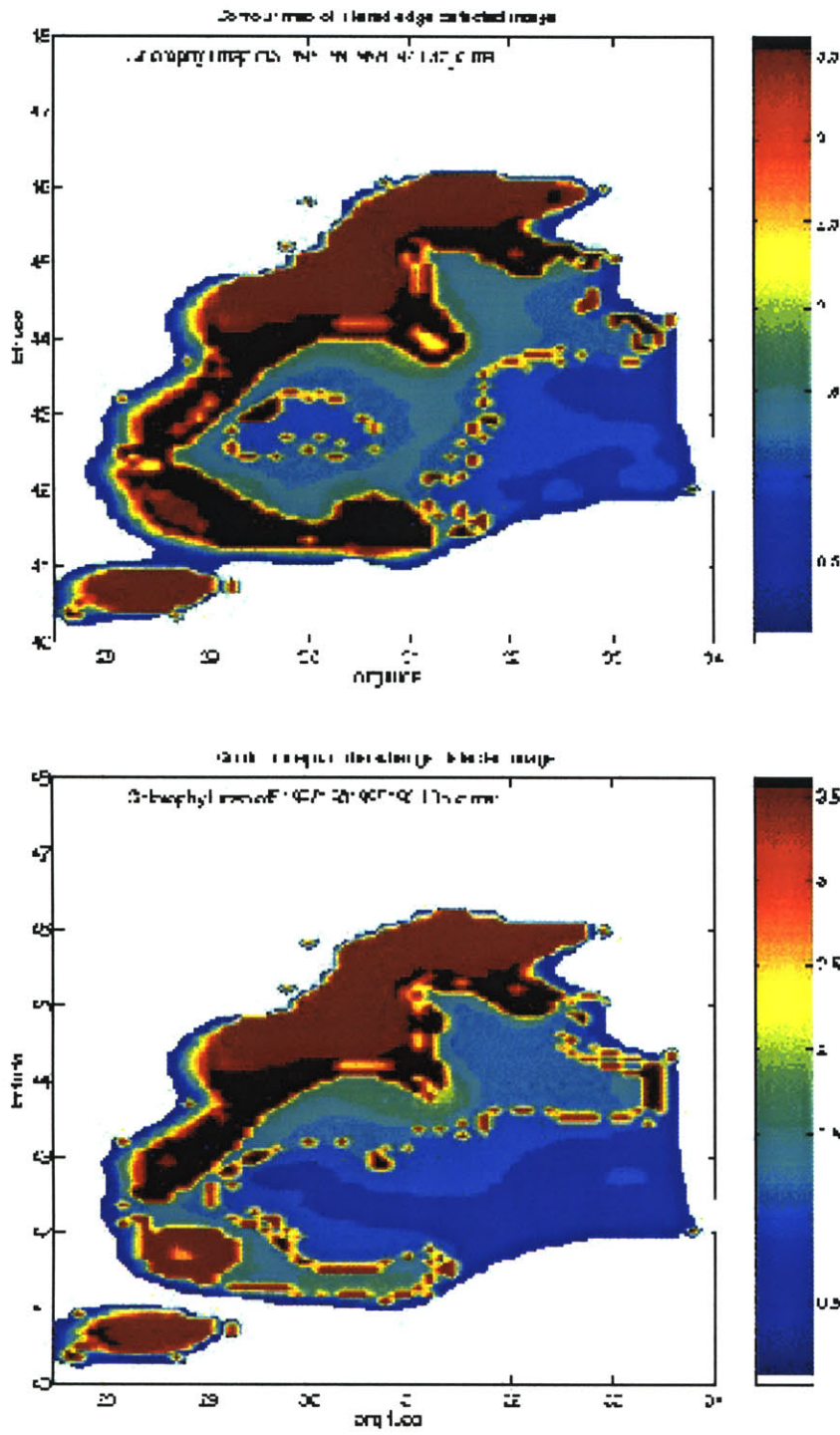
Figure 6-7: Chlorophyll maps from July 1998.
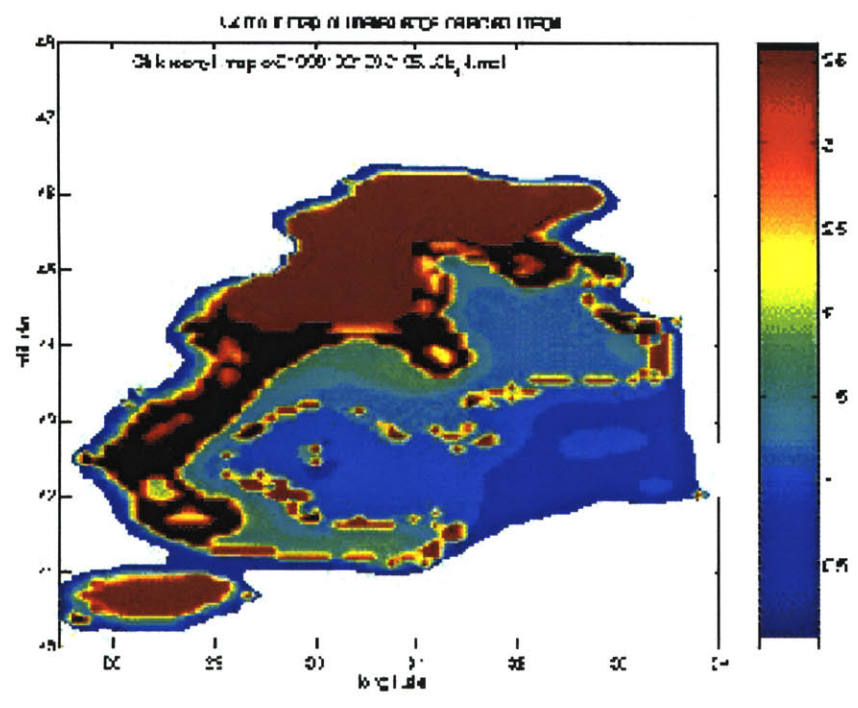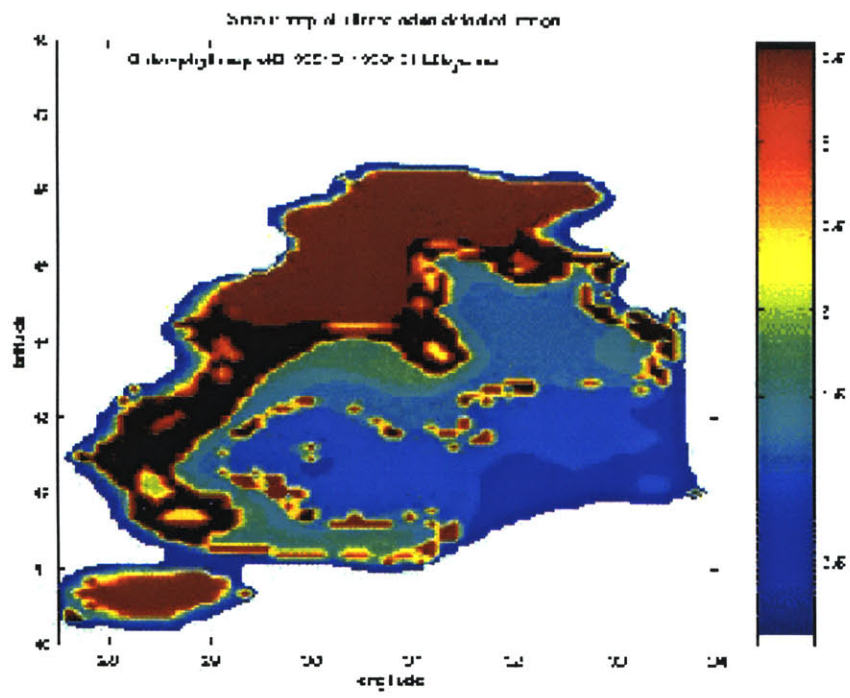
Figure 6-8: Chlorophyll maps from July 1998.
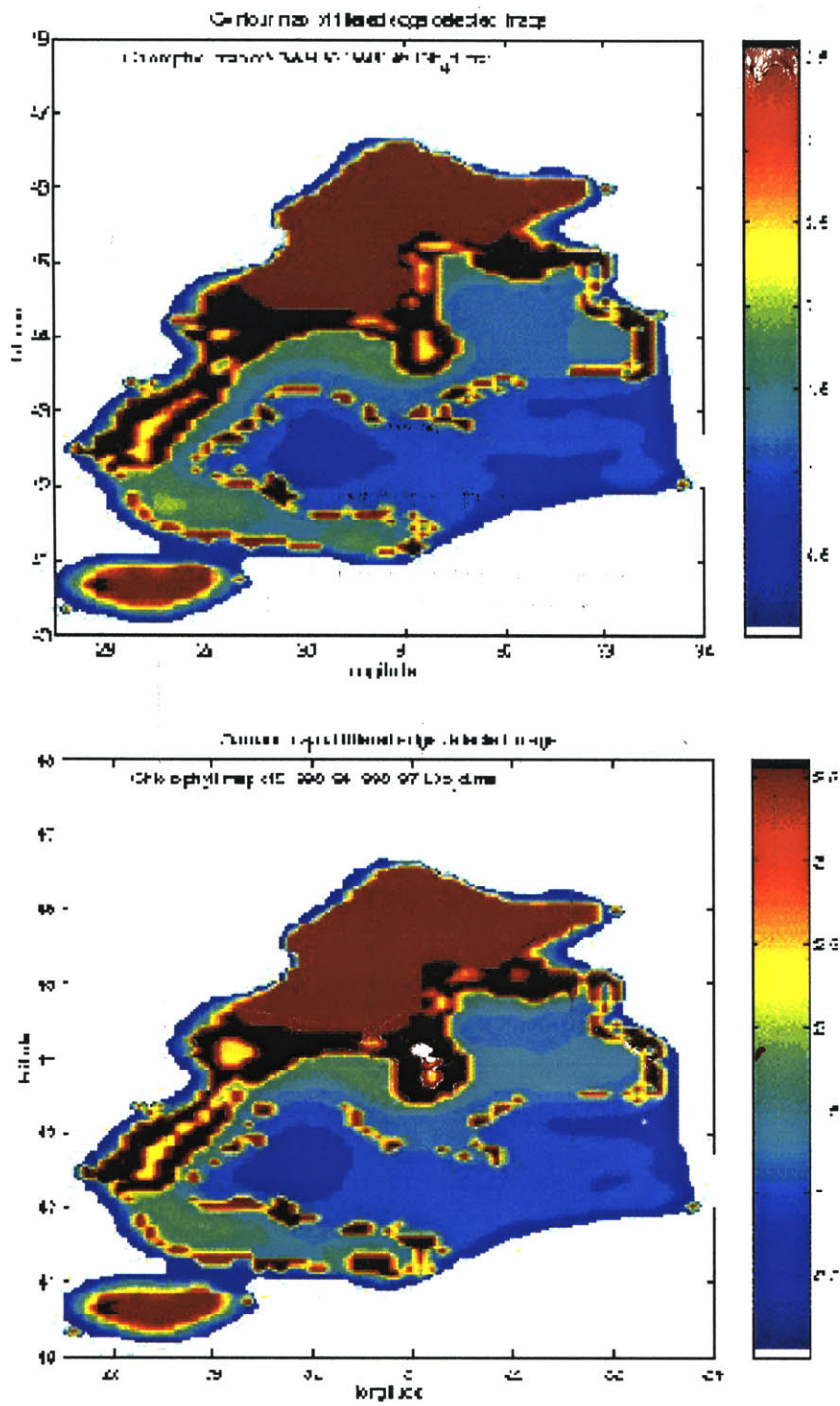
Figure 6-9: Chlorophyll maps from July 1998.
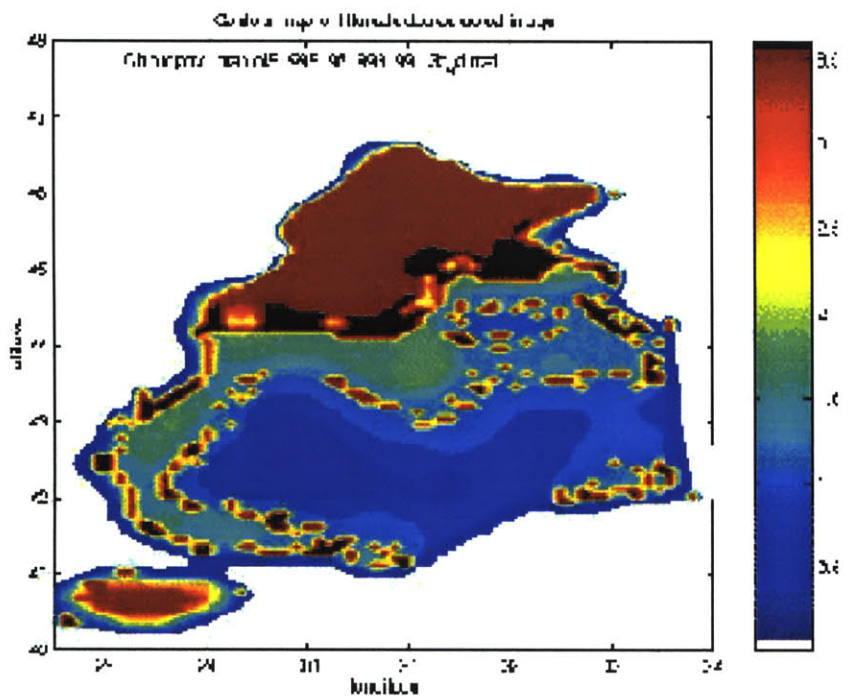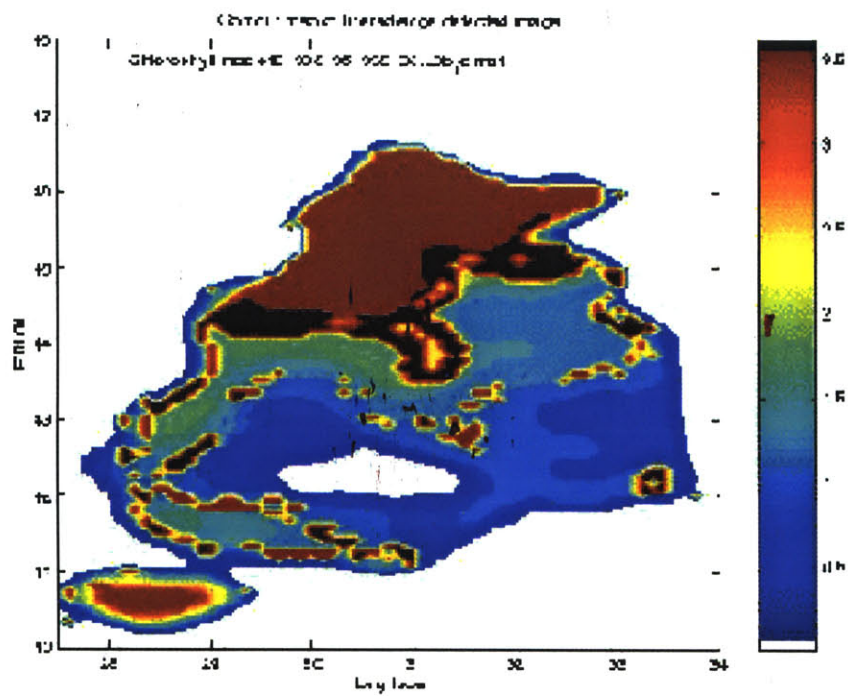
Figure 6-10: Chlorophyll maps from July 1998. The previous 6 figures show the formation of a finger-like structure extending out from the high chlorophyll region of water toward the center of the Sea.
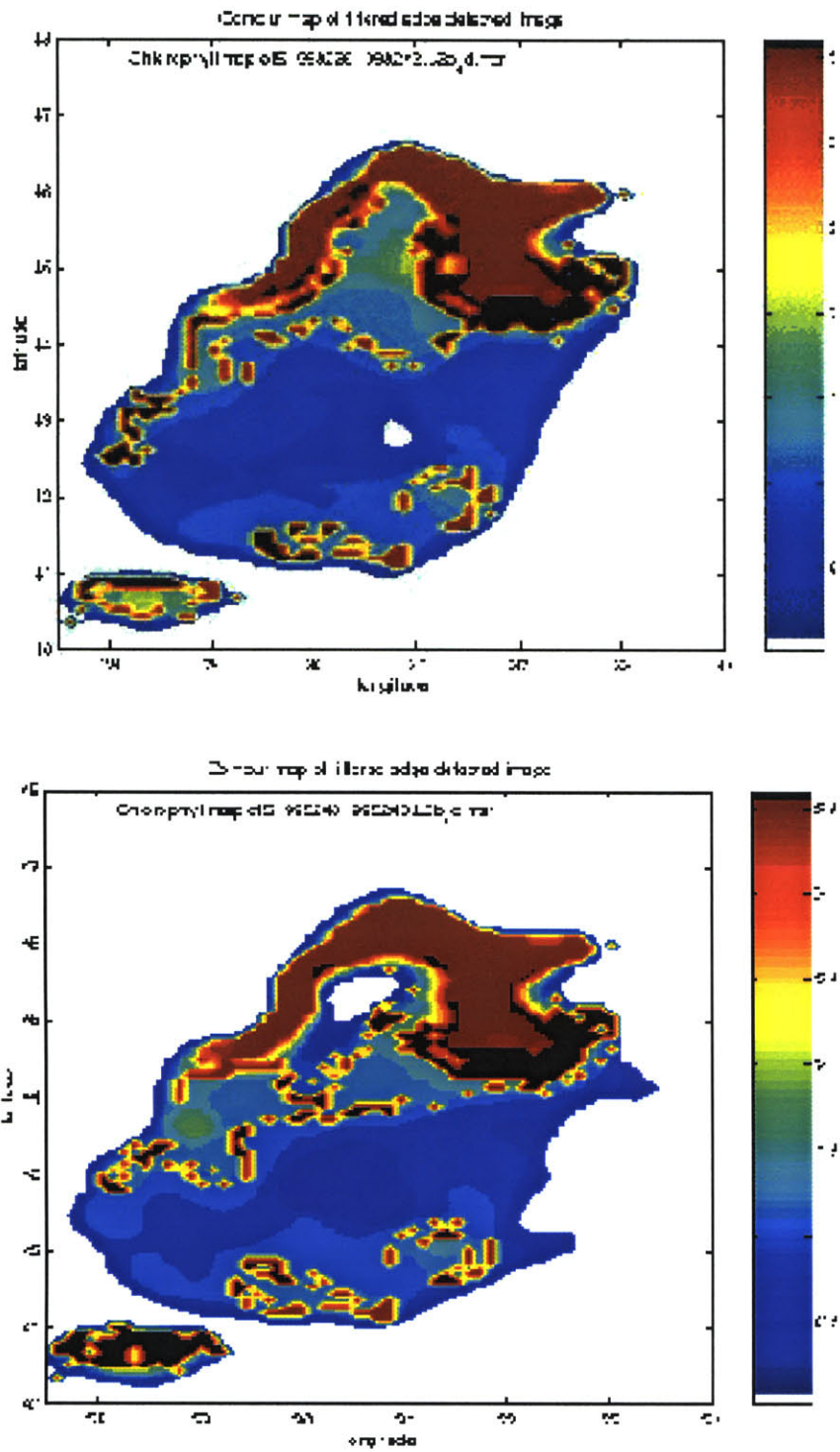
Figure 6-11: Chlorophyll maps from September 1998 when the chlorophyll is at a low along the western coast.
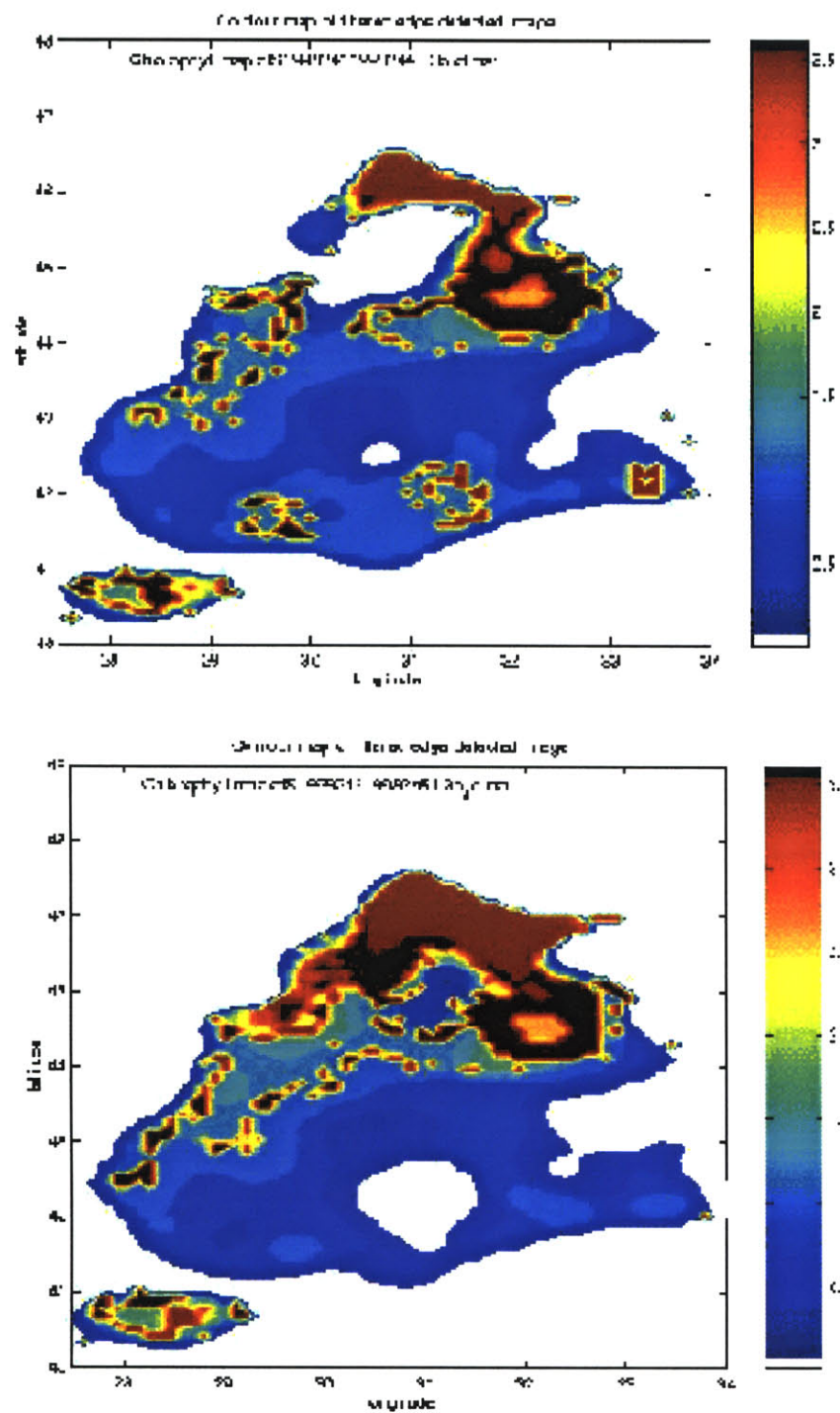
Figure 6-12: Chlorophyll maps from September 1998 when the chlorophyll is at a low along the western coast.
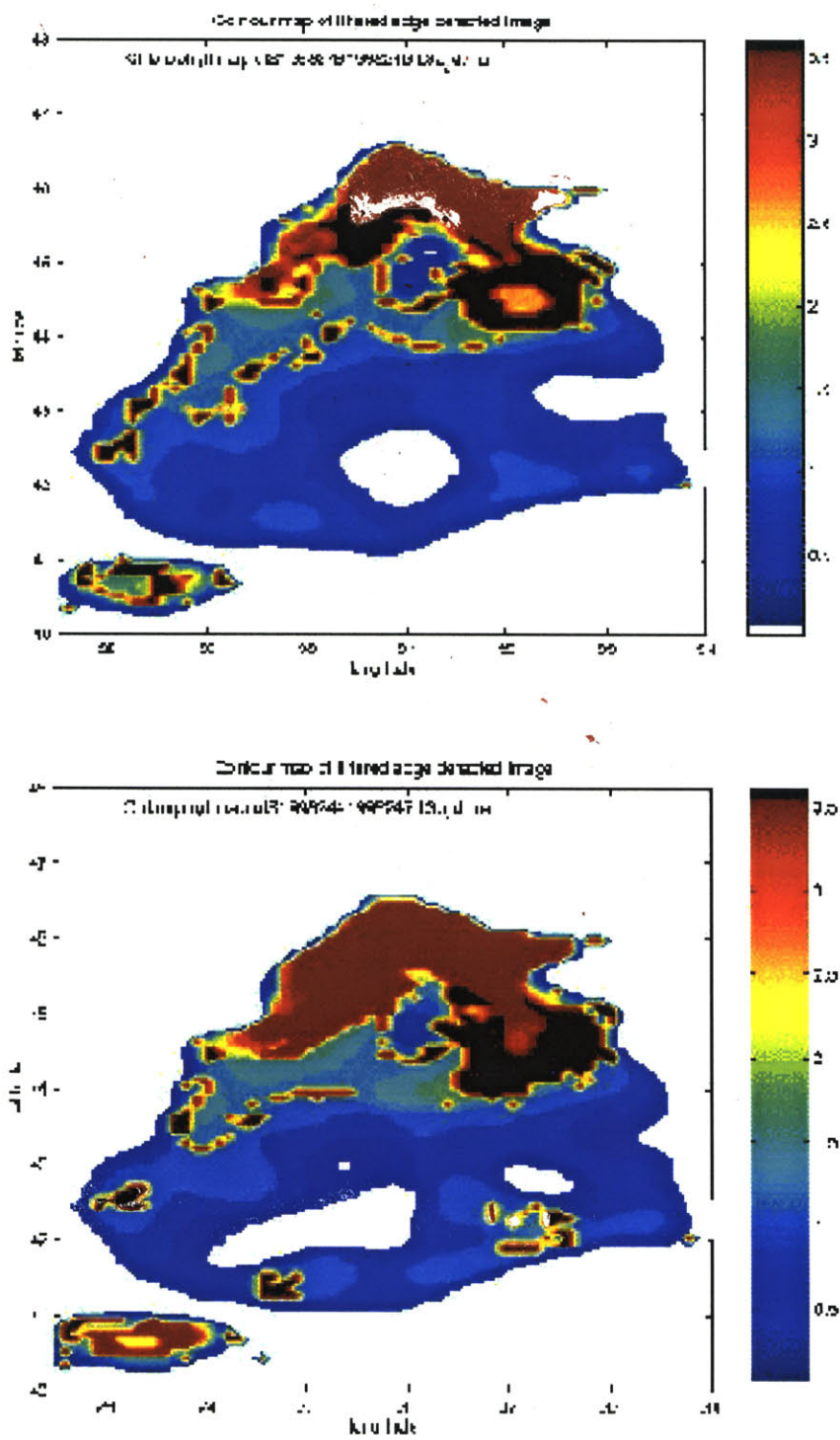
Figure 6-13: Chlorophyll maps from September 1998 when the chlorophyll is at a low along the western coast.
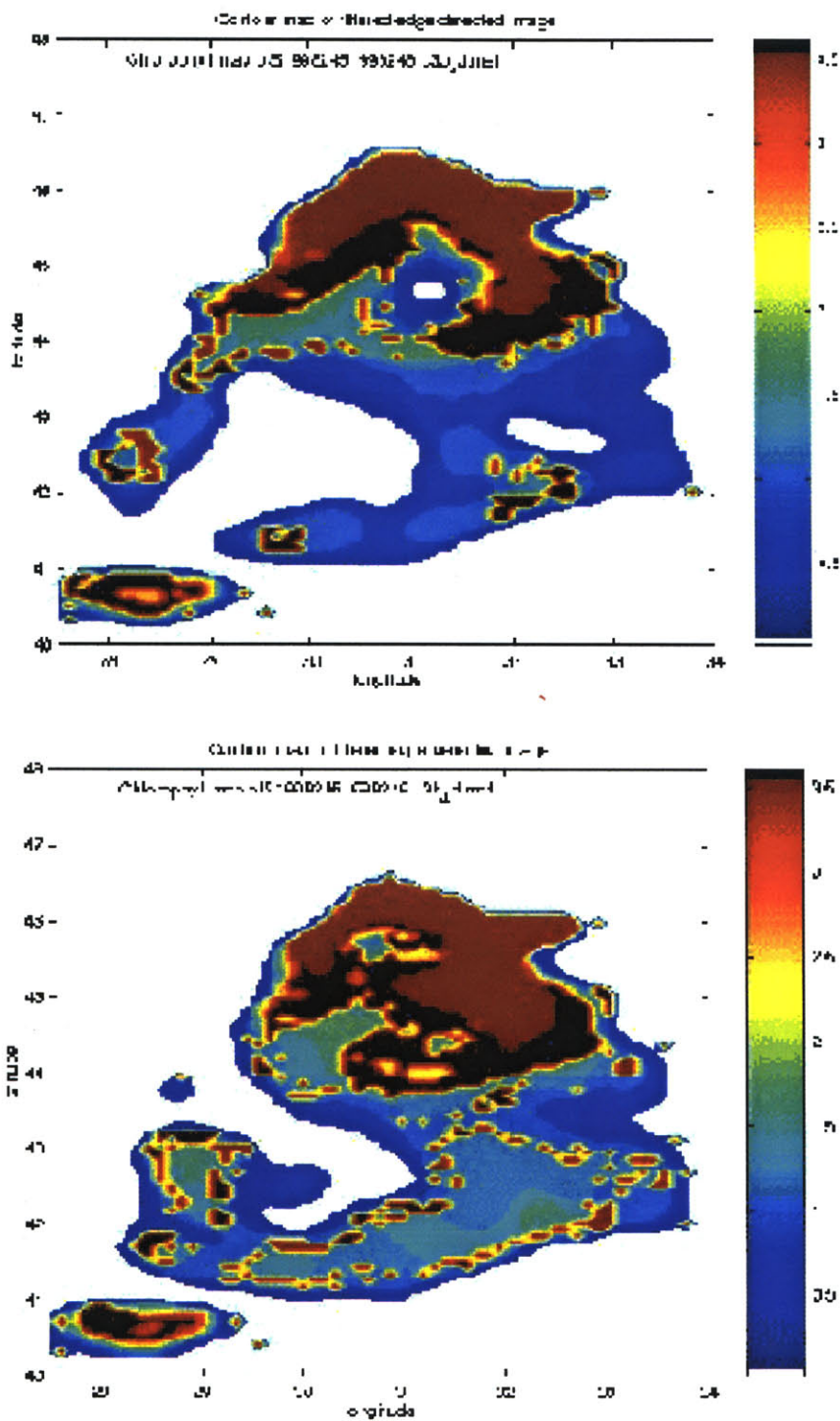
Figure 6-14: Chlorophyll maps from September 1998 when the chlorophyll is at a low along the western coast.
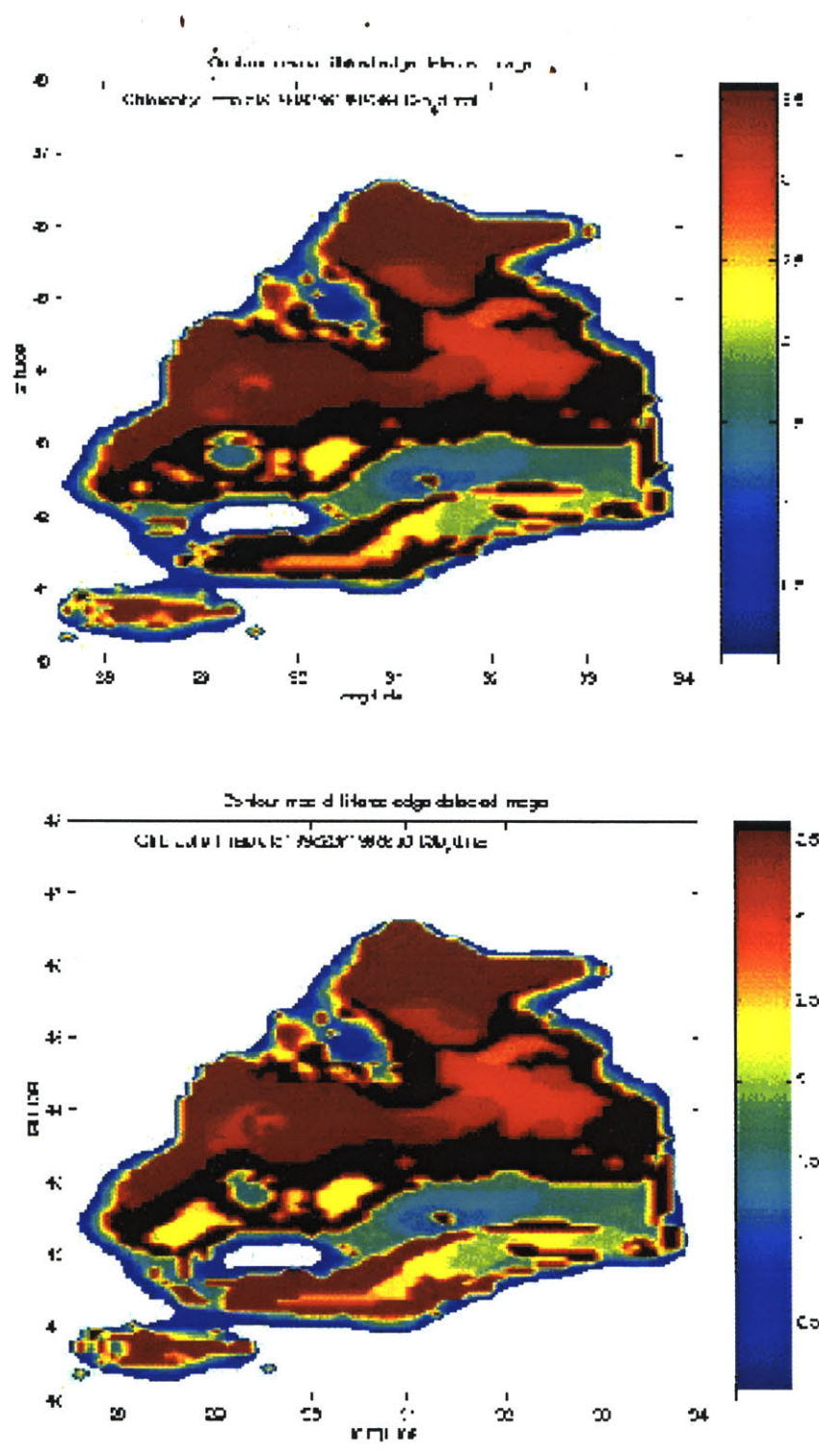
Figure 6-15: Chlorophyll maps from October of 1998 when large blooms engulf the western Black Sea.
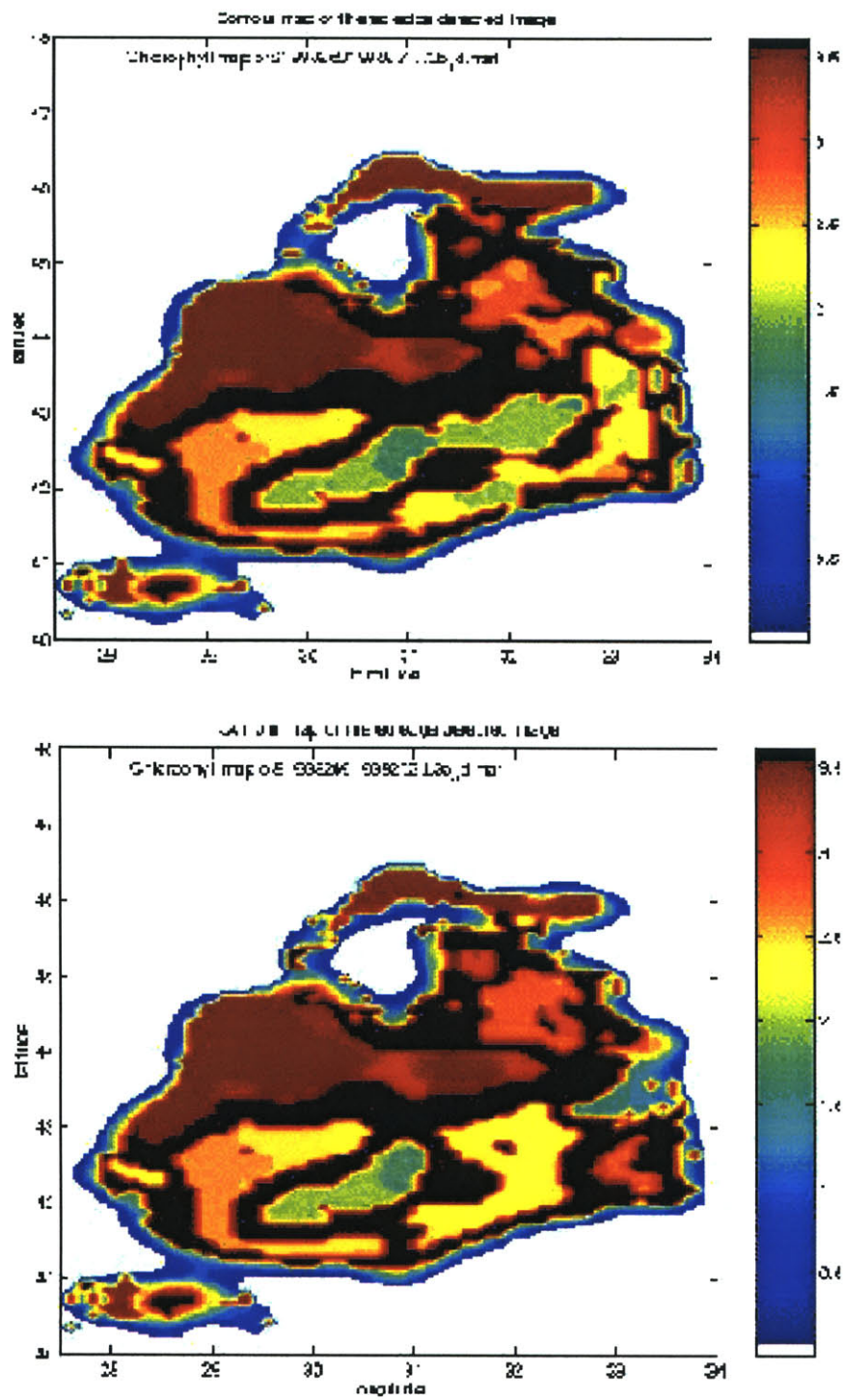
Figure 6-16: Chlorophyll maps from October 1998 when large blooms engulf the western Black Sea.
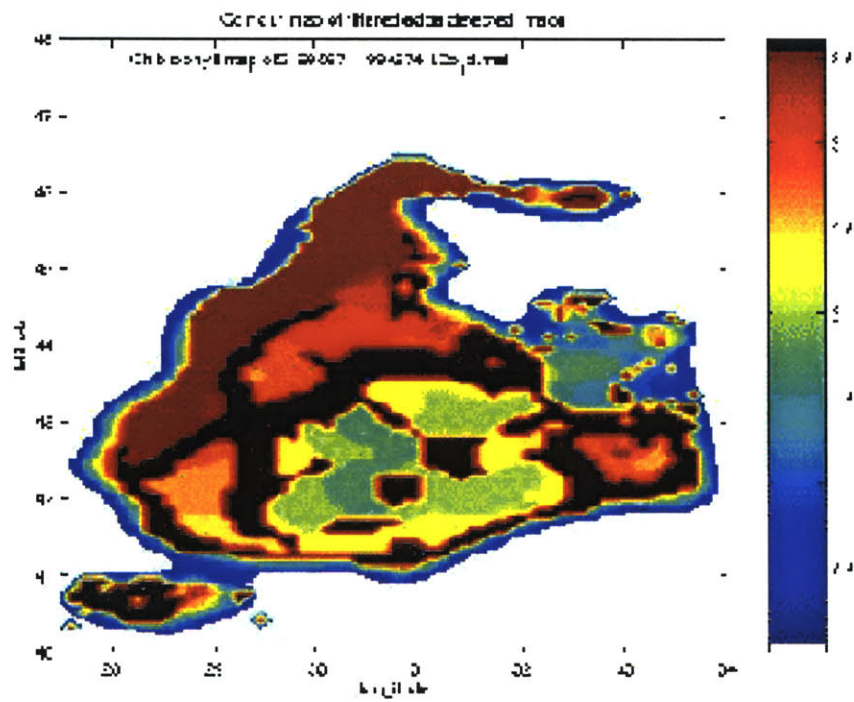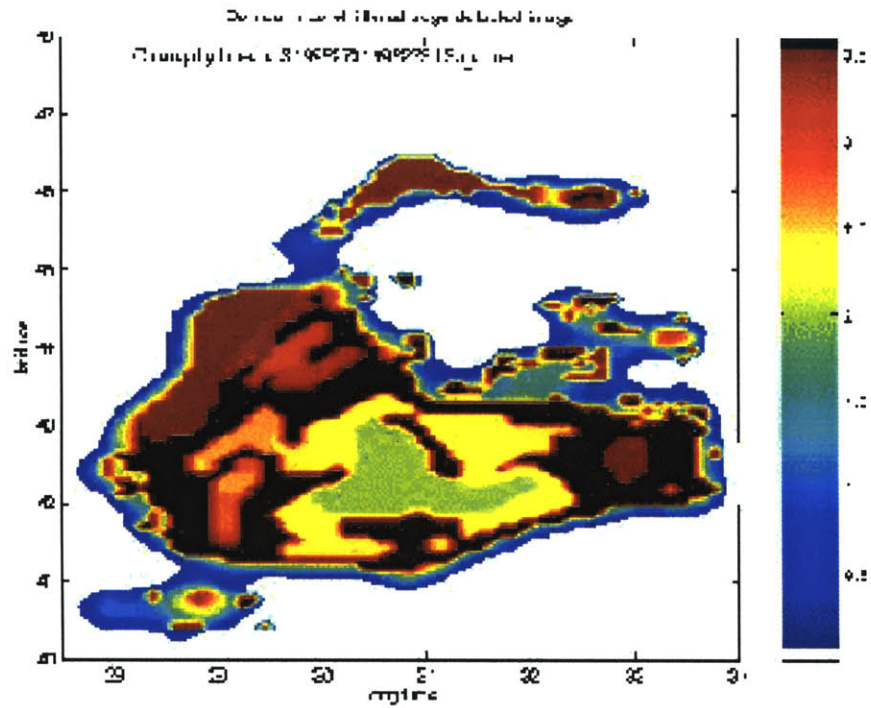
Figure 6-17: Chlorophyll maps from October 1998 when large blooms engulf the western Black Sea.
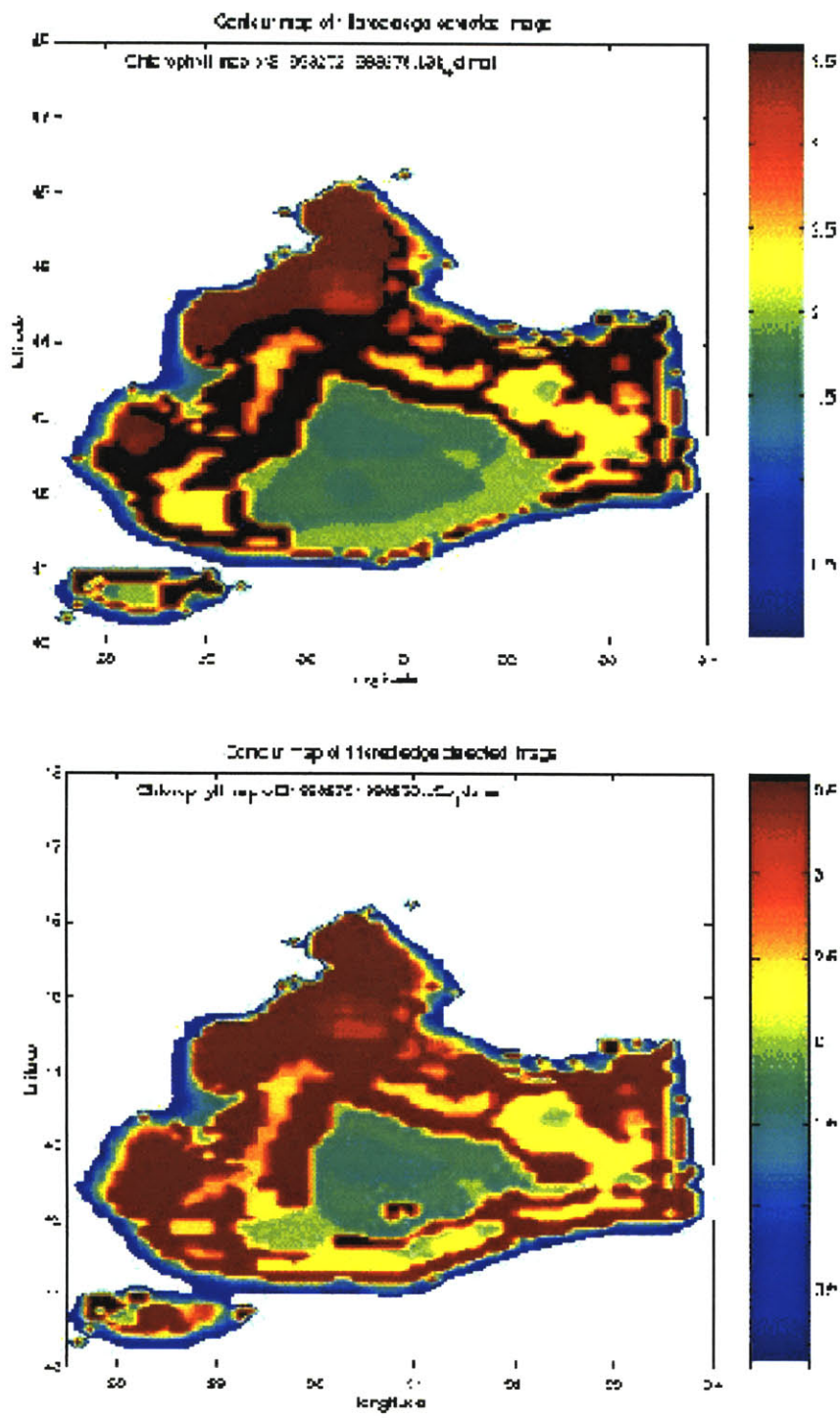
Figure 6-18: Chlorophyll maps from October 1998 when large blooms engulf the western Black Sea.
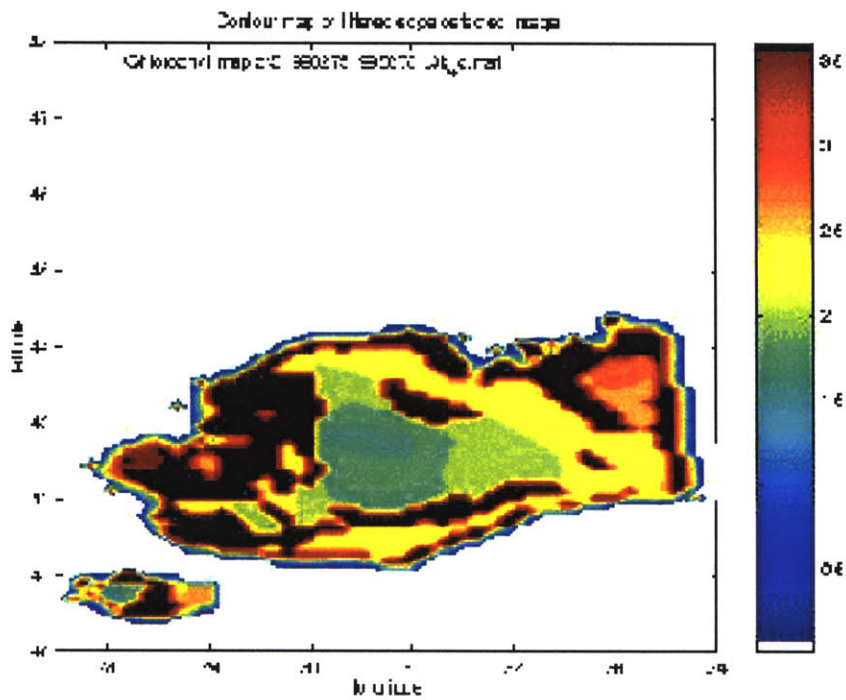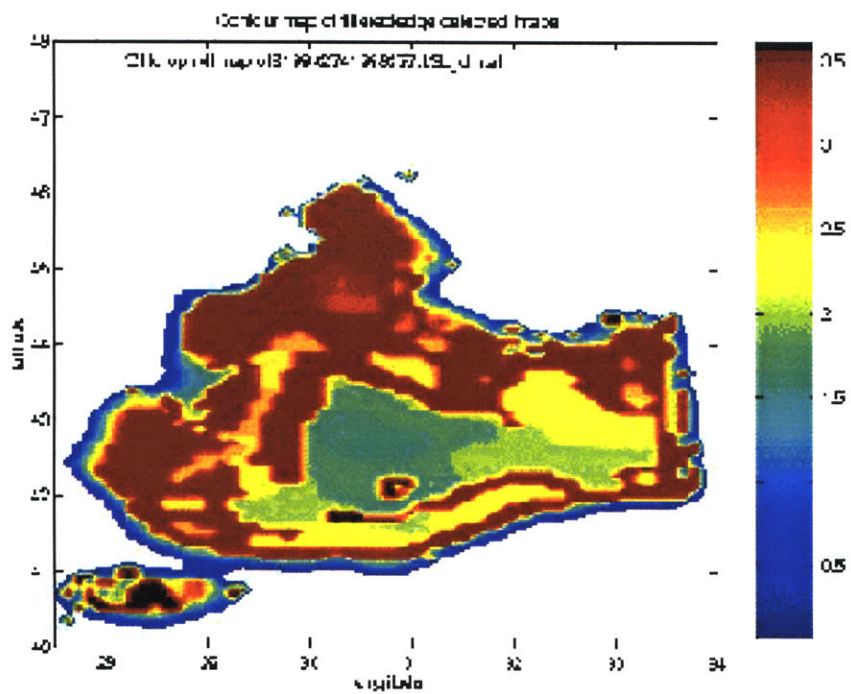
Figure 6-19: Chlorophyll maps from October 1998 when large blooms engulf the western Black Sea.
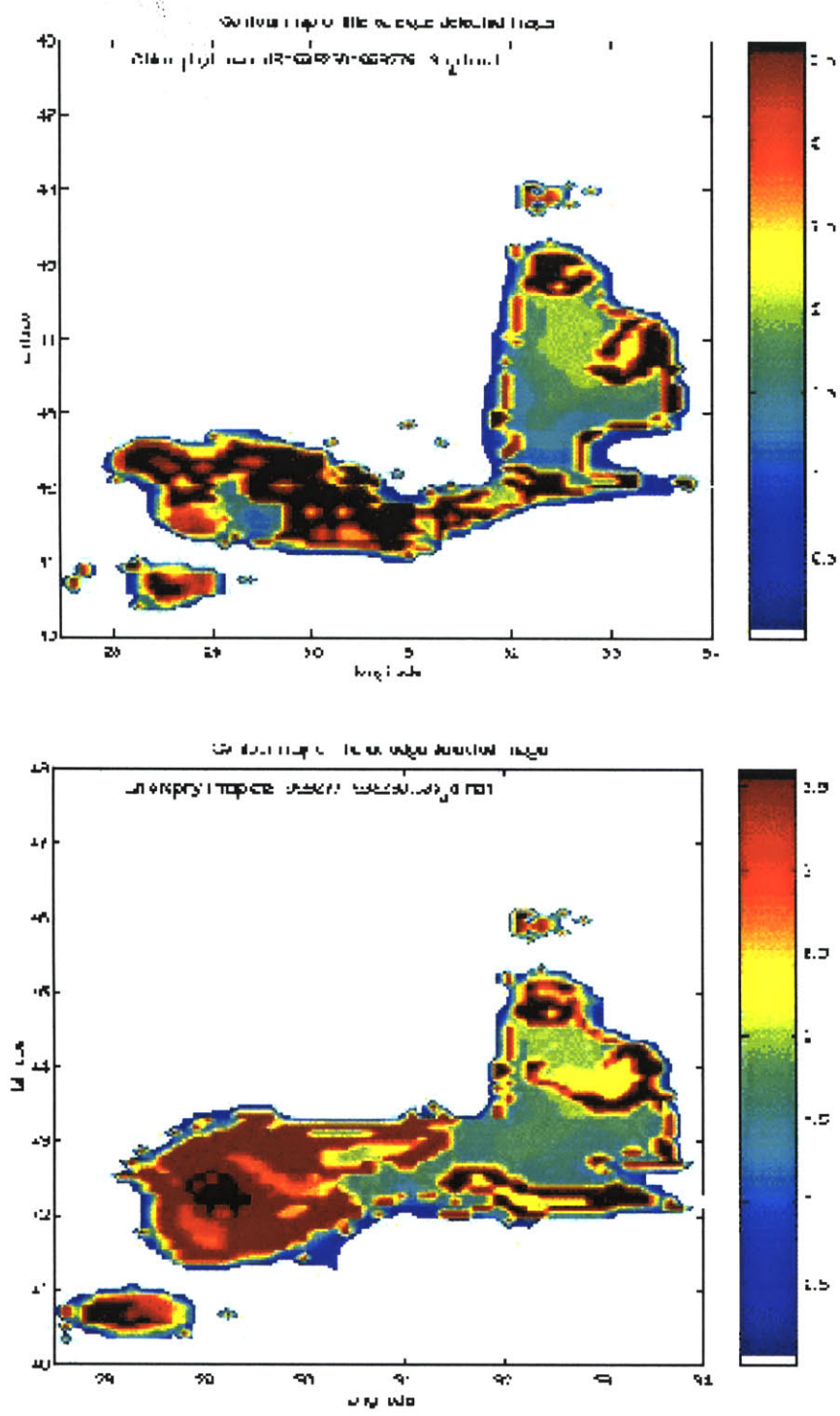
Figure 6-20: Chlorophyll maps from October 1998 when large blooms engulf the western Black Sea.
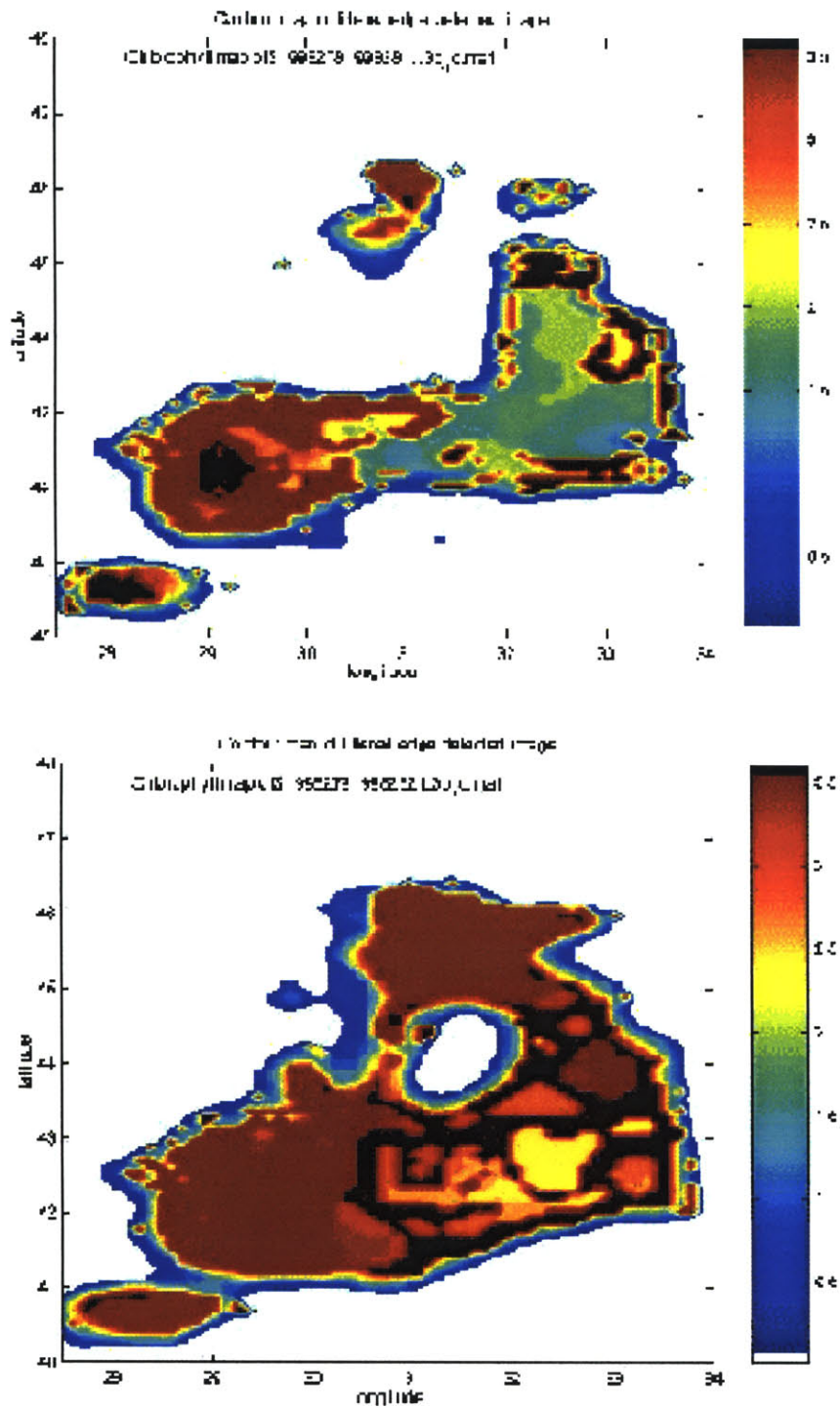
Figure 6-21: Chlorophyll maps from October 1998 when large blooms engulf the western Black Sea.

Chapter 7

Future Work

While the edge detection algorithm works with reasonable success, it does have areas that need improvement. The edges that are detected by the algorithm tend to to be thick and obscure data values in the chlorophyll maps. Thinning these edges would benefit the analysis of gradient properties around fronts.

Also, the application of this algorithm and subsequent analysis of data for additional years would be of scientific benefit. Implementation on additional data will also test the robustness and universality of the algorithm. Additional data will also determine whether the properties seen in the Summer of 1998 in the Black Sea are unique to that time period or if the features occur with regularity in the summertime.

The use of the edge detection algorithm on other ocean color data sets such as CZCS and MODIS would also benefit the study of the Black Sea. The analysis of CZCS data will reveal information of how the nature of blooms associated with the Danube has changed over time. Beginning work with MODIS data, which was launched in December 1999 on the Terra Satellite, will set the foundation for analysis in the future .

Chapter 8

Conclusion

There is considerable seasonal variability in the amount of location and presence of chlorophyll in the Northwestern Black Sea. This is, in part, due to the influence of the Danube River. Changes in the outflow of the river are reflected in the location and shape of chlorophyll blooms.

The edge detection algorithm described in this thesis can successfully delineate a region of high chlorophyll from the surrounding low chlorophyll waters. This high chlorophyll region is a water mass that contains a significant amount of the nutrient rich water from Danube outflow. Mushroom structures and other circulation features can be observed and delineated by edge analysis.

Unfortunately, there are instances in which the edge detection algorithm fails on this data set. This is likely to be a result of the thresholding portions of the algorithm. While the thresholds are necessary to suppress noise-related edges, they also prevent the detection of steep edges. In other cases, the edges are very broad or have gaps. This problem may be solved using a thinning and interpolation algorithm.

Overall, this edge detection algorithm is a promising means of automatically identifying features in the Black Sea. It well identifies the influence of the Danube on the circulation of the shelf. The identification of this water mass can be useful for the study of the effect of high nutrient water flux into the Black Sea and in order to track its movement.

Appendix A

Appendix A

A.1 MATLAB code to breakdown Hierchial Data Format (HDF) SeaWiFS Level 3 Binned data files

at10.0pt *%This is a program to be used in order to breakdown HDF files in MATLAB*
%It is a culmination of considerable effort.
%Latest Revision at7.0pt at5.0pt at10.0pt at7.0pt at5.0pt at10.0pt at7.0pt at5.0pt—— 3/7/00
%Ashwini Deshpande
%Note, original code was acquired from Stephanie Dutkiewicz

%Change directory to location of daily data files
cd /usr/seawifs/dayave/;

%   10
% READ GLOBAL ATTRIBUTES
% (see pg 49–51 of SeaWifs "Operational archive product
%   specifications" for descriptions)
%
%
% access file to read global attirbutes
sd_id=hdfsd at10.0pt('start', [namefile,'.main'],'rdonly');

71

```
at10.0ptif (sd_id==-1), 'problem opening file (sd-mode)', end
%
attr_index=hdfsd('findattr',sd_id,'Product Name');                          20
[ga_product_name, status]=hdfsd('readattr',sd_id,attr_index);
ga_product_name
attr_index=hdfsd('findattr',sd_id,'Start Year');
[ga_start_year, status]=hdfsd('readattr',sd_id,attr_index);
attr_index=hdfsd('findattr',sd_id,'Start Day');
[ga_start_day, status]=hdfsd('readattr',sd_id,attr_index);
attr_index=hdfsd('findattr',sd_id,'End Year');
[ga_end_year, status]=hdfsd('readattr',sd_id,attr_index);
attr_index=hdfsd('findattr',sd_id,'End Day');
[ga_end_day, status]=hdfsd('readattr',sd_id,attr_index);                     30
attr_index=hdfsd('findattr',sd_id,'Northernmost Latitude');
[ga_northmost, status]=hdfsd('readattr',sd_id,attr_index);
attr_index=hdfsd('findattr',sd_id,'Southernmost Latitude');
[ga_southmost, status]=hdfsd('readattr',sd_id,attr_index);
attr_index=hdfsd('findattr',sd_id,'Westernmost Longitude');
[ga_westmost, status]=hdfsd('readattr',sd_id,attr_index);
attr_index=hdfsd('findattr',sd_id,'Easternmost Longitude');
[ga_eastmost, status]=hdfsd('readattr',sd_id,attr_index);
attr_index=hdfsd('findattr',sd_id,'Data Bins');
[ga_data_bins, status]=hdfsd('readattr',sd_id,attr_index);                   40
attr_index=hdfsd('findattr',sd_id,'Percent Data Bins');
[ga_percent_bins, status]=hdfsd('readattr',sd_id,attr_index);


% close access to file
status=hdfsd('end',sd_id);
if (status==-1), 'problem closing file (sd-mode)', end



% clean up
clear attr_index sd_id                                                      50


% open main file
file_id=hdfh('open', [namefile,'.main'],'rdonly',0);
```

```matlab
if (file_id==-1), 'problem opening file', end
% start v-interface
status=hdfv('start',file_id);
if (status==-1), 'problem opening v-interface', end


% find data
    vdata_ref=hdfvs('findclass',file_id,'Index');                          60
    if (vdata_ref==0), 'problem finding Index vdata', end


    if (vdata_ref>0),


% open vdata
        vdata_id=hdfvs('attach',file_id,vdata_ref,'r');


% find out what is in data and set up to read
        [n_index, interlace, fields, nbytes, vdata_name, status] = ...
            hdfvs('inquire',vdata_id);                                     70
        vdata_name
        if (status==-1), 'problem inquiring about vdata', end
        status = hdfvs('setfields',vdata_id,fields);
        if (status==-1), 'problem setting fields', end


% read vdata
        [data, index_count]=hdfvs('read',vdata_id,n_index);
        in_row_num=data{1,1};   %index of row
        in_vsize=data{2,1};     %n-s extent of bins in each row
        in_hsize=data{3,1};     %e-w extent of bins in each row            80
        in_start_num=data{4,1}; %number of first bin in each row
        in_begin=data{5,1};     %first data-containing bin in each row
        in_extent=data{6,1};    %number of data-containing bins in each row
        in_max=data{7,1};       %maximum number of bins in each row


% close vdata
        status=hdfvs('detach',vdata_id);
        if (status==-1), 'problem closing Index vdata', end
% clean up
```

73

```
    clear data n interlace fields nbytes vdata_name status vdata_id                    90
end
% find data
 vdata_ref=hdfvs('findclass',file_id,'DataMain');
 if (vdata_ref==0), 'problem finding List vdata', end
%
 if (vdata_ref>0),
% open vdata
    vdata_id=hdfvs('attach',file_id,vdata_ref,'r');
% find out what is in data and set up to read
    [n_list, interlace, fields, nbytes, vdata_name, status] = ...           100
         hdfvs('inquire',vdata_id);


    vdata_name
    if (status==-1), 'problem inquiring about vdata', end
    status = hdfvs('setfields',vdata_id,fields);
    if (status==-1), 'problem setting fields', end


% read vdata

                                                                             110

    [data, index_count]=hdfvs('read',vdata_id,n_list);
%          display('got through that.  Pheww');
    li_bin_num=data{1,1};       %index number of each d-c bin
    li_nobs=data{2,1};          %number observations in each d-c bin
%   li_nscenes=data{3,1};        %number scenes contributing to each bin
%   li_time_rec=data{4,1};       %time distribution of binned data
%   li_weights=data{5,1};        %sum of weights of input data
%   li_sel_cat=data{6,1};        %selection catagory
%   li_flags_set=data{7,1};      %corresponds to parent L2 products
                                                                             120

% close vdata
    status=hdfvs('detach',vdata_id);
    if (status==-1), 'problem closing List vdata', end


% clean up
```

```
    clear data n interlace fields nbytes vdata_name status vdata_id
end
```

```
%
% ---------------------------------------------------130--------
% |    read Subordinate vdata                        |
% |    ------------------------                              |
% | sum and sum_square data for each data-containing bin      |
% | (data length is number of data-containing bins: <5 940 422)|
% | (same number as in List vdata)                   |
% ------------------------------------------------------------
%
```

```
% find required data                                                    140
% vdata_ref=hdfvs('findclass',file_id,'DataSubordinate');
% if (vdata_ref==0), 'problem finding Subordinate vdata', end
  vdata_ref=hdfvs('find',file_id,'nLw_412');
  if (vdata_ref==0), 'problem finding czcs pigment vdata', end
%
  if (vdata_ref>0),
% open vdata^M
    vdata_id=hdfvs('attach',file_id,vdata_ref,'r');
% find out what is in data and set up to read
    [n_sub, interlace, fields, nbytes, vdata_name, status] = ...           150
        hdfvs('inquire',vdata_id);
    vdata_name
    if (status==-1), 'problem inquiring about vdata', end
    status = hdfvs('setfields',vdata_id,fields);
    if (status==-1), 'problem setting fields', end
% read vdata
    [data, index_count]=hdfvs('read',vdata_id,n_sub);
    if (index_count<0),
      'did not read subordinate data, check subordinate file is in this directory', else
      su_sum = data{1,1};    %sum of natural logs of binned pixel values      160
      su_sum_sq = data{2,1};  %sum of squares of natural log
```

75

end *%if^M*

% close vdata^M

   status=hdfvs('detach',vdata_id);

   if (status==−1), 'problem closing Subordinate vdata', **end**

% clean up

   clear data n interlace fields nbytes vdata_name status vdata_id

end *%if*

% save subordinate data

save l3b_oct_412_whole.mat su_sum

clear su_sum su_sum_sq

% −

%

vdata_ref=hdfvs('find',file_id,'nLw_443');

  if (vdata_ref==0), 'problem finding czcs pigment vdata', **end**

%

  if (vdata_ref>0),

% open vdata

   vdata_id=hdfvs('attach',file_id,vdata_ref,'r');

% find out what is in data and set up to read

   [n_sub, interlace, fields, nbytes, vdata_name, status] = ...

      hdfvs('inquire',vdata_id);

   vdata_name

   if (status==−1), 'problem inquiring about vdata', **end**

   status = hdfvs('setfields',vdata_id,fields);

   if (status==−1), 'problem setting fields', **end**

% read vdata^M

   [data, index_count]=hdfvs('read',vdata_id,n_sub);

   if (index_count<0),

    'did not read subordinate data, check subordinate file is in this directory', **else**

    su_sum = data{1,1};   *%sum of natural logs of binned pixel values*

    su_sum_sq = data{2,1}; *%sum of squares of natural log*

   end *%if*

```matlab
% close vdata
   status=hdfvs('detach',vdata_id);
   if (status==-1), 'problem closing Subordinate vdata', end        200
% clean up
clear data n interlace fields nbytes vdata_name status vdata_id
end


% save subordinate data
save l3b_oct_443_whole.mat su_*


clear su_sum su_sum_sq


% remove subordinate file from this directory                       210
%----------------------------------------------------------------------
%


vdata_ref=hdfvs('find',file_id,'nLw_490');
 if (vdata_ref==0), 'problem finding czcs pigment vdata', end
%
 if (vdata_ref>0),
% open vdata
   vdata_id=hdfvs('attach',file_id,vdata_ref,'r');
% find out what is in data and set up to read                       220
   [n_sub, interlace, fields, nbytes, vdata_name, status] = ...
       hdfvs('inquire',vdata_id);
   vdata_name
   if (status==-1), 'problem inquiring about vdata', end
   status = hdfvs('setfields',vdata_id,fields);
   if (status==-1), 'problem setting fields', end
% read vdata
   [data, index_count]=hdfvs('read',vdata_id,n_sub);
   if (index_count<0),
      'did not read subordinate data, check subordinate file is in this directory', else   230
      su_sum = data{1,1};     %sum of natural logs of binned pixel values
      su_sum_sq = data{2,1};  %sum of squares of natural log
   end %if
```

77

```
% close vdata
   status=hdfvs('detach',vdata_id);
   if (status==−1), 'problem closing Subordinate vdata', end
% clean up
clear data n interlace fields nbytes vdata_name status vdata_id
end
```
240
```
% save subordinate data
save l3b_oct_490_whole.mat su_*


clear su_sum su_sum_sq


% remove subordinate file from this directory
%−−−−−−−−−−−−−−−−−−−−−−−−−−−−−−−−−−−−−−−−−−−−−−−−−−−−−−−−
%


vdata_ref=hdfvs('find',file_id,'nLw_510');                            250
   if (vdata_ref==0), 'problem finding czcs pigment vdata', end
%
   if (vdata_ref>0),
% open vdata
   vdata_id=hdfvs('attach',file_id,vdata_ref,'r');
% find out what is in data and set up to read
   [n_sub, interlace, fields, nbytes, vdata_name, status] = ...
        hdfvs('inquire',vdata_id);
   vdata_name
   if (status==−1), 'problem inquiring about vdata', end       260
   status = hdfvs('setfields',vdata_id,fields);
   if (status==−1), 'problem setting fields', end
% read vdata
   [data, index_count]=hdfvs('read',vdata_id,n_sub);
   if (index_count<0),
      'did not read subordinate data, check subordinate file is in this directory', else
      su_sum = data{1,1};     %sum of natural logs of binned pixel values
      su_sum_sq = data{2,1};  %sum of squares of natural log
   end
```

78

% close vdata

status=hdfvs('detach',vdata_id);

if (status==−1), 'problem closing Subordinate vdata', **end**

% clean up

clear data n interlace fields nbytes vdata_name status vdata_id

end

% save subordinate data

save l3b_oct_510_whole.mat su_*

clear su_sum su_sum_sq

% remove subordinate file from this directory

%−−

%

vdata_ref=hdfvs('find',file_id,'nLw_555');

  if (vdata_ref==0), 'problem finding czcs pigment vdata', **end**

%

  if (vdata_ref>0),

% open vdata

    vdata_id=hdfvs('attach',file_id,vdata_ref,'r');

% find out what is in data and set up to read

    [n_sub, interlace, fields, nbytes, vdata_name, status] = ...

        hdfvs('inquire',vdata_id);

    vdata_name

    if (status==−1), 'problem inquiring about vdata', **end**

    status = hdfvs('setfields',vdata_id,fields);

    if (status==−1), 'problem setting fields', **end**

% read vdata

    [data, index_count]=hdfvs('read',vdata_id,n_sub);

    if (index_count<0),

      'did not read subordinate data, check subordinate file is in this directory', **else**

      su_sum = data{1,1};   *%sum of natural logs of binned pixel values*

      su_sum_sq = data{2,1}; *%sum of squares of natural log*

    end *%if*

% close vdata

```
    status=hdfvs('detach',vdata_id);
    if (status==−1), 'problem closing Subordinate vdata', end
```
% clean up
```
clear data n interlace fields nbytes vdata_name status vdata_id
```
end

% save subordinate data
```
save l3b_oct_555_whole.mat su_*
```

```
clear su_sum su_sum_sq
```

%————————————————————————————————————

%remove chloraphyll−a

```
vdata_ref=hdfvs('find',file_id,'chlor_a');
    if (vdata_ref==0), 'problem finding czcs pigment vdata', end
```
%
```
    if (vdata_ref>0),
```
% open vdata
```
    vdata_id=hdfvs('attach',file_id,vdata_ref,'r');
```
% find out what is in data and set up to read
```
    [n_sub, interlace, fields, nbytes, vdata_name, status] = ...
        hdfvs('inquire',vdata_id);
    vdata_name
    if (status==−1), 'problem inquiring about vdata', end
    status = hdfvs('setfields',vdata_id,fields);
    if (status==−1), 'problem setting fields', end
```
% read vdata^M
```
    [data, index_count]=hdfvs('read',vdata_id,n_sub);
    if (index_count<0),
        'did not read subordinate data, check subordinate file is in this directory', else
        su_sum = data{1,1};    %sum of natural logs of binned pixel values
        su_sum_sq = data{2,1};  %sum of squares of natural log
    end %if
```
% close vdata

310

320

330

340

80

```
        status=hdfvs('detach',vdata_id);
        if (status==-1), 'problem closing Subordinate vdata', end
% clean up
clear data n interlace fields nbytes vdata_name status vdata_id
end


% save subordinate data
save l3b_oct_chl_a_whole.mat su_*
```

```
clear su_sum su_sum_sq


%-----------------------------
%CZCS pigment


vdata_ref=hdfvs('find',file_id,'CZCS_pigment');
    if (vdata_ref==0), 'problem finding czcs pigment vdata', end
%
    if (vdata_ref>0),
% open vdata
        vdata_id=hdfvs('attach',file_id,vdata_ref,'r');
% find out what is in data and set up to read
        [n_sub, interlace, fields, nbytes, vdata_name, status] = ...
            hdfvs('inquire',vdata_id);
        vdata_name
        if (status==-1), 'problem inquiring about vdata', end
        status = hdfvs('setfields',vdata_id,fields);
        if (status==-1), 'problem setting fields', end
% read vdata
        [data, index_count]=hdfvs('read',vdata_id,n_sub);
        if (index_count<0),
         'did not read subordinate data, check subordinate file is in this directory', else
         su_sum = data{1,1};     %sum of natural logs of binned pixel values
         su_sum_sq = data{2,1};  %sum of squares of natural log
        end %if
% close vdata
        status=hdfvs('detach',vdata_id);
```

if (status==−1), 'problem closing Subordinate vdata', **end**

% clean up

clear data n interlace fields nbytes vdata_name status vdata_id   380

end

% save subordinate data

save l3b_oct_CZCS_pig_whole.mat su_*

clear su_sum su_sum_sq

% remove subordinate file from this directory

%− −

% close v−interface   390

  status=hdfv('end',file_id);

 if (status==−1), 'problem closing v-interface', **end**

%

% close main file

  status=hdfh('close',file_id);

 if (status==−1), 'problem closing file', **end**

%

% clean up

  clear ans file_id index_count status vdata_ref

%   400

% save bin and time data

  save l3b_oct.mat ga_* li_* in_begin in_extent

% save subordinate data

*% save l3b_oct_su.mat su_**

%

% save l3b index data

save l3b_in.mat in_hsize in_max in_row_num in_start_num in_vsize

                                                                             410

420

Appendix B

Appendix B

B.1   MATLAB code to edge detect chlorophyll maps

% Program Name: Edge_finder.m

% Author: Ashwini G. Deshpande

% Last Update: 4/12/2000

%Clear Memory

clear

%Change Directory to data location

cd /usr/seawifs/matfiles/junjul

%

%Set it up automation. Will process all files in a directory.   10

fnames=ls('*.mat');

sfns=size(fnames)

fn1=1

fn2=27

j=1

while fn2 <= sfns(2)

cd /usr/seawifs/matfiles/junjul

mat1=fnames(fn1:fn2);

%Load Data   20

```matlab
load(mat1);
cd ~/thesis
la=size(nmat);
inc=1;
%Set up for Contour Plots
ay=linspace(40,48,la(1));
fay=linspace(48,40,la(1));
ax=linspace(27.5,34,la(2));
v=[.01 .5 .65 .8 1 1.2 1.4 1.6 1.8 2 2.2 2.4 2.6 2.8 3 3.2 3.4 3.5 3.6];        30


%Wiener Filter raw data
fmat1=wiener2(nmat,[4 4]);


%Median Filter wiener filtered data
fmat=medfilt2(fmat1,[5 5]);


%Set up Sobel Edge detection filters
%Vertical gradients
soby=[1 2 1 ; 0 0 0 ; -1 -2 -1];                                                40
%Horizontal gradients
sobx=-soby' ;


%Threshold data

subsat=find(fmat > 3.3);
fmat(subsat)=3.3;
fmat1(subsat)=3.3;

subsat=find((fmat >= 1.2) & (fmat <= 2.0));                                      50
fmat(subsat)=2;
fmat1(subsat)=2;

subsat=find((fmat < 1.2) & (fmat>=.1));
fmat(subsat)=1;
fmat1(subsat)=1;
```

clear subsat

%High Pass filter data
sub_mat=(fmat1−fmat);

%Smooth results to eliminate noise caused results
sub_mat=medfilt2(sub_mat,[2,2]);

%All this smoothing causes the map shape to blur.   This step stops that.
lost=find((sub_mat == 0) & nmat);
sub_mat(lost)=.01;
lost=find((sub_mat)&(nmat == 0));
sub_mat(lost)=0;

clear lost

%Add back high frequency edges.   Edge enhancement
addback=zeros(size(sub_mat));
weights=find(sub_mat >= .3);
addback(weights)=sub_mat(weights);
sfmat=fmat+addback;

clear fmat addback weights

%Apply Sobel Edge Detector
hzed=filter2(sobx,sfmat);
vted=filter2(soby, sfmat);
maged=(hzed.ˆ2)+(vted.ˆ2);

clear hzed vted

%Reconstruct again.
lost=find((maged == 0) & nmat);
maged(lost)=.01;
lost=find((maged)&(nmat == 0));
maged(lost)=0;

clear lost

%Apply thresholding to find edges of interest

dkeep=find((nmat < 1.2) & (nmat));

maged(dkeep)=.01;

100

clear dkeep

%Find gradients that correspond to edges with thresholding.

kick=find(maged >=19);

maged(kick)=.01;

kick=find((maged <=.3) &(maged));

maged(kick)=.01;

clear kick

110

clear fmat1

%To make superimposed plots

%Creat Plots

super=medfilt2(wiener2(nmat,[4 4]),[5 5]);

tbs=find(super >=3.5);

super(tbs)=3.5;

120

impose=find(maged > .01);

super(impose)=3.6;

%figure

colormap('default');

ct=zeros(66,3);

ct(2:65,:)=colormap;

ct(1,:)=[1 1 1];

colormap(ct);

contourf(ax,ay,super,v)

shading flat

xlabel('`longitude`')

ylabel('`latitude`')

text(28.2,47.5,['Chlorophyll map of', mat1]);

title('`Contour map of filtered edge detected image`')^M

colorbar

hold off

clear super impose tbs

%To make movies.

M(j)=getframe;

%to make Postscript files and printouts

cd /usr/seawifs/psfiles

fn=strcat(mat1(1:23), '`ps`');

print('`-dpsc`', fn)

print('`-dpsc`', '`-Pcolor-4-035`')

cd ~/thesis

%go to next file in directory.

fn1=fn1+27;

fn2=fn2+27;

j=j+1;

end

Appendix C

Appendix C

C.1 MATLAB code to create 4 day running averages

```
%Program Name: autoave4.m
%Author: ashwini deshpande
%Last udated: 2/21/2000


%new program to make 4 day averages



cd /usr/seawifs/dayave/daymat99/;

%Set up data grid                                                    10
chldat4=zeros(96,61,4);
totave=4;

%Automate and load data of each of 4 days into chldat4
fnames=ls('S*.mat');
szf=size(fnames);
%length of filenames is 20 characters
ct1=1;
ct2=21;
```

```
while (3*21)+ct2 <= szf(2)                                                    20
        cntr=1;
        while cntr <= totave
                ct1t=ct1+(21*(cntr−1));
                ct2t=ct1t+20;
                mat1=(fnames(ct1t:ct2t));
                load(mat1)
                lgt=length(latsave);
                n=1;
                l=1;
                m=1;                                                          30
                while n<=lgt
                        nlat=latsave(n);
                        countdat(l,m)=datchl(n);
                    n=n+1;
                        if n <= lgt
                                tlat=latsave(n) ;
                                if tlat ~= nlat
                                        l=l+1;
                                        m=1;
                                end                                           40
                        end
                        m=m+1;
                end
                chldat4(:,:,cntr)=countdat;
                cntr=cntr+1;
        end
        iv=1;
        ih=1;


%Do the averaging                                                             50
        nmat=countdat;
        numuse=countdat;
        while iv <=96
                while ih <= 61
                        minmat=chldat4(iv,ih,:);
```

```
minmat=reshape(minmat,4,1);
nbad=find(minmat==0);
if length(nbad) < 4
        gta=find(minmat);
        ave4d=mean(minmat(gta));                              60
        nmat(iv,ih)=ave4d;
        numuse(iv,ih)=4−length(nbad);
    else
        nmat(iv,ih)=0;
        numuse(iv,ih)=0;
    end
    ih=ih+1;
    end
    ih=1;
    iv=iv+1;                                                  70
end


%Store new binary files
    cd /usr/seawifs/matfiles/junjul99/
    fnamep1=fnames(ct1:ct1+7);
    fnamep2=int2str(str2double(fnames(ct1+1:ct1+7))+3);
    fname=strcat(fnamep1,fnamep2,'.L3b_4d','.mat');
    save(fname, 'nmat', 'numuse');
    fname
    cd /usr/seawifs/dayave/daymat99/                          80
    ct1=ct1+21;
    ct2=ct2+20;
end
```

Bibliography

[1] James G. Acker. Volume 22: The heritage of SeaWiFS: A retrospecitive on the CZCS NIMBUS experiment team (NET) progam. Technical Report 104566, NASA, September 1994.

[2] Janet W. Campbell, John M. Blaisdell, and Michael Darzi. Volume 32: Level-3 SeaWiFS data products: Spatial and temporal binning algorithms. Technical Report 104566, NASA, August 1995.

[3] Jean-Francios Cayula and Peter Cornillon. Edge detection algorithm for sst images. *Journal of Atmospheric and Oceanic Technology*, 9(1):67—80, February 1992.

[4] Gene Feldman. SeaWiFS project — software and documentation. Web Page, February 2000. http://seawifs.gsfc.nasa.gov/SEAWIFS/SOFTWARE/SOFTWARE.html.

[5] Gene Carl Feldman. An overview of SeaWiFS and the SeaStar spacecraft. Web Page, February 2000. http://seawifs.gsfc.nasa.gov/SEAWIFS/SEASTAR/SPACECRAFT.html.

[6] Gene Carl Feldman. SeaWiFS project — background. Web Page, February 2000. http://seawifs.gsfc.nasa.gov/SEAWIFS/BACKGROUND/SEAWIFS_BACKGROUND.html.

[7] Ronald J. Holyer and Sarah H. Peckinpaugh. Edge detection applied to satellite imagery of the oceans. *IEEE Transactions on Geoscience and Remote Sensing*, 27(1):46–56, January 1989.

[8] Steve Kemplar. GDAAC-MDL-01 002 ges distributed active archive center verison 1.0. Web Page, February 2000. http://daac.gsfc.nasa.gov.

[9] National Academy of Sciences of Ukraine. Ibss nasu. black sea. ctenophora. mnemiopsis leidyi. Web Page, April 2000. http://www.ibss.iuf.net/blacksea/species/freelife/ctenophora/mnemleid.html.

[10] US Glocal Ocean Flux Study Office. Ocean color from space. Web Page, February 2000. http://daac.gsfc.nasa.gov/CAMPAIGN_DOCS/OCDST/ocean_color_from_space.html.

[11] Temel Oguz et al. Mesoscale circulation and thermohaline structure of the black sea observed during hydroblack '91. *Deep Sea Research*, 41(4):603–628, 1994.

[12] Temel Oguz and Paola Malanotte-Rizzoli. Seasonal variability of wind and thermohaline-driven circulation in the black sea: Modeling studies. *Journal of Geophysical Research*, 101(C7):16551—16569, July 1996.

[13] John E. O'Reilly, Stephane Maritorena, B. Gregg Mitchell, David A. Siegel, Kendall L. Carder, Mati Kahru, and Charles McClain. Ocean color chlorophyll algorithms for SeaWiFS. *Journal of Geophysical Research*, 103(C11):24937—24953, October 1998.

[14] Black Sea Web Project. Blackseaweb. Web Page, April 2000. http://www.blackseaweb.net/.

[15] Kevin George Ruddick, Fabrice Ovidio, and Machteld Rijkeboer. Atmospheric correction of SeaWiFS imagery for turbid coastal and inland waters. *Applied Optics*, 39(6):897—912, February 2000.

[16] Emil Stanev. On the mechanisms of the black sea circulation. *Earth-Science Reviews*, 28:285–319, 1990.

[17] Yu. Zaitsev and V. Mamaev. *Marine Biological Diversity in the Black Sea — A Study of Change and Decline.* United Nations Publications, New York, 1997.